CHALMERS
UNIVERSITY OF TECHNOLOGY

Analysis and Study of Self-driving bikes

Master's thesis in Mobility Engineering

Brijesh Kuduva Prakash
Harish Jayachandran

DEPARTMENT OF ELECTRICAL ENGINEERING

CHALMERS UNIVERSITY OF TECHNOLOGY
Gothenburg, Sweden 2024
www.chalmers.se

Master's thesis 2024

Analysis and Study of Self-driving bikes

Brijesh Kuduva Prakash
Harish Jayachandran

CHALMERS
UNIVERSITY OF TECHNOLOGY

Department of Electrical Engineering
Chalmers University of Technology
Gothenburg, Sweden 2024

Analysis and Study of Self-driving bikes
Brijesh Kuduva Prakash, Harish Jayachandran

Supervisor: Carina Björnsson, Volvo Cars
Supervisor: Jonas Sjöberg, Professor in Electrical Engineering
Examiner: Jonas Sjöberg, Professor in Electrical Engineering

Master's Thesis 2024
Department of Electrical Engineering
Chalmers University of Technology
SE-412 96 Gothenburg
Telephone +46 31 772 1000

Cover: Electric Scooter (e-scooter) used in the project

Typeset in LaTeX
Gothenburg, Sweden 2024

Analysis and Study of Self-driving bikes
Brijesh Kuduva Prakash, Harish Jayachandran
Department of Electrical Engineering
Chalmers University of Technology

Abstract

Advancements in vehicle technologies and their active safety systems have necessitated various testing methods to ensure safety and reliability. Traditional methods using stationary bikes or simple mobile platforms lack realistic behaviour as compared to a bicyclist. Testing for bikes is crucial as cycling is a major mode of transportation for the general population. The increase in bicycles [1] and e-scooter usage [2], prompts Original equipment manufacturers, to decrease and mitigate the safety risks for these users termed as vulnerable road users. The Self-driving bike project aims to bridge this gap by developing bikes and e-scooter that mimic human riding behavior. These create realistic test scenarios to evaluate vehicle safety systems which is supported by a collaboration with Volvo Cars. This thesis contributes to the development of self-driving bikes and e-scooters by focusing on areas, including the remodelling of the steering motor mount for the e-scooter for improved durability, addressing cable management issues, and designing a 3D-printed roller for indoor testing of the e-scooter. Fine-tuning the steering motor through ESCON Studio and calibrating the motor contributed to optimize the steering angle range. The configuration and setting up of self-driving bikes and e-scooter for field tests at Astazero, collecting and analyzing data to refine performance along with an analysis of indoor and outdoor tests, focusing on balance, steering rates, and other performance metrics under various conditions. These contributions enhance the testing mechanisms for self-driving bikes and e-scooter, bridging the gap between stationary methods and real-world scenarios.

Keywords: Simulations, Analysis, Self-driving bikes, E-scooters, Testing.

Acknowledgements

We would like to thank Jonas Sjöberg, our examiner and supervisor at Chalmers University of Technology, for his invaluable guidance, insightful feedback, and continuous encouragement. We are also deeply grateful to Carina Björnsson, our supervisor at Volvo Cars Corporation, for her expert advice and unwavering support to carry out the work. Our sincere thanks to Erik Ronelöv and Peter N Eriksson for their assistance with booking and guidance at the Astazero test track, which was crucial for the practical aspects of this project. We extend our gratitude to Armin Khorsandi for generously sharing his knowledge of the project and previous work. Special thanks to our family and friends for their love and and support, which were invaluable during this process. Finally, we would like to acknowledge Chalmers University of Technology and Volvo Cars Corporation for providing the resources and facilities necessary to complete our thesis.

Brijesh Kuduva Prakash and Harish Jayachandran, Gothenburg, November 2024

List of Acronyms

The list of acronyms used in the report are listed in alphabetical order:

AEB	Automatic Emergency Braking
AD	Autonomous Driving
ADAS	Advanced Driver Assistance Systems
CAD	Computer Aided Design
CoM	Centre of Mass
CPA	Closest Point Algorithm
GPS	Global Positioning System
IMU	Inertial Measurement Unit
LKA	Lane Keeping Aid
LQR	Linear Quadratic Regulator
PD	Proportional Derivative
RAB	Rear Automatic Braking

Contents

List of Figures

List of Tables

1
Introduction

1.1 Problem Background

As urban populations grow and environmental concerns prompt a shift towards sustainable transportation, cycling and the usage of e-scooters has emerged as a popular mode of travel [1] [2]. However, this increase has highlighted a significant challenge: ensuring the safety of vulnerable road users in environments dominated by motor vehicles. The interaction between bikes/e-scooters and cars presents unique risks that necessitate targeted safety measures. Statistics of fatalities with cyclists has shown no decline in the past decade in the European Union [3].

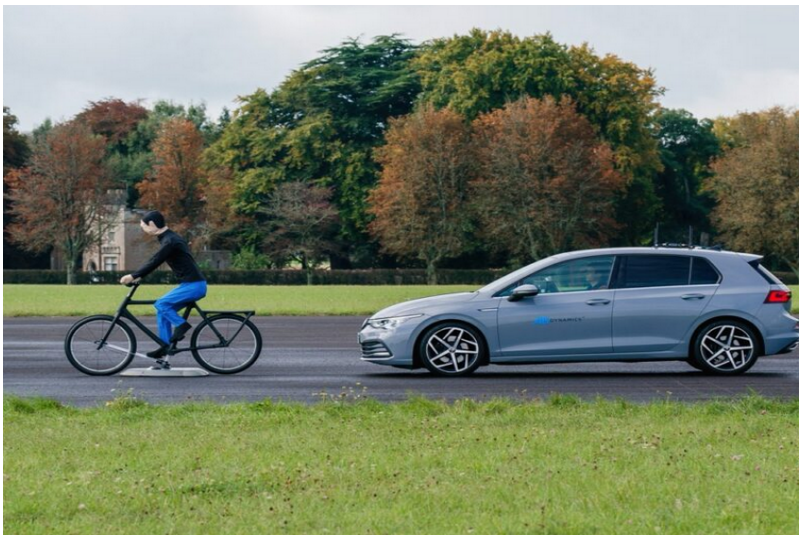

Figure 1.1: Interaction between test objects in a controlled environment [4]

To address the risks presented by the interaction between bikes and cars, a crucial step is the testing of these interactions in controlled, safe environments as shown in Figure 1.1. Testing for near crash scenarios in real life such as a bike joining a busy interaction where a possible collision with a car can occur is one such example. Tests like these can provide valuable data and insights that lead to the development of effective safety measures. By leveraging virtual simulations, real-world tests, and advanced technologies, researchers can gain a comprehensive understanding of the risks and identify strategies to mitigate them. This approach not only enhances the safety of vulnerable road users but also contributes to the creation of a more sustainable and inclusive transportation system.

At Chalmers University of Technology along with Volvo Cars, we commenced work with bicycles as part of the Self-driving bike project, which began in 2017. The project's objective is to develop a self-driving bike that can replicate the behavior of a traditional bike, including balancing and following a predetermined path. These autonomous bicycles are intended for testing alongside cars. Since its inception, various students have contributed to the project, resulting in the development of multiple bikes and an e-scooter.

Traditional methods using stationary bikes or mobile platforms lack the realism required for effective testing for example leaning in curves is a maneuver that can only be performed by a real biker but real bikers cannot be used for testing due to safety reasons. A target is needed to be used and the development of a target and its ability to mimic a real biker are essential, which leads to the development of self-driving bikes. The Self-Driving Bike project aims to bridge this gap by developing bikes and e-scooter that mimic human riding behavior. These create realistic test scenarios to evaluate vehicle safety systems which is supported by a collaboration with Volvo Cars, and Astazero provided the track to perform the tests.

1.2 Volvo Cars Corporation and Autobike Project

Volvo Cars regards safety as their highest priority. The modern three-point safety belt was perfected by Volvo engineer Nils Bohlin in 1959 and its patent was given for free to the world. The invention has been credited with saving at least a million lives worldwide [6]. To reach the best safety standards, modern Volvo cars are equipped with sensors like Radar, Camera, Lidar, etc. These sensors help with the perception of the Car along with its assistance in car's Active safety functions such as Automatic Emergency Braking (AEB), Lane keeping Aid (LKA), Rear Automatic Braking (RAB) in low speeds.

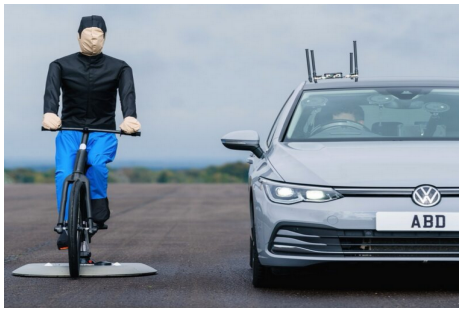

(a) Test car and test bike with a dummy[4]

(b) Test bike with a dummy on a mobile platform [5]

Figure 1.2: Test objects

These functions have to be validated to ensure safety. They are tested and validated in controlled environments like in a test track. This thesis work is performed under the Collision avoidance team at Volvo cars. This team is responsible for testing

and validating two main active safety functions namely, AEB and LKA. For testing these functions, many test objects are used such as soft vehicles, test dummy, and test bikes as seen in the Figure 1.2.

Although, these mobile platforms were successful in testing the vehicle's active safety functions, there were a few disadvantages:

1. Scenario representation: The mobile platforms struggle to mimic real-world bike scenarios like wiggling or leaning in the curves.
2. Target representation: Self-driving bikes provide a more realistic target representation for evaluating sensors and control systems as compared to the mobile platforms.

To achieve accurate and precise testing of the vehicle's safety functions, the Autobike project and Volvo Cars partnered to use self-driving bikes as test objects. The bikes must be able to repeat the same path to achieve robustness in testing. Therefore, the bikes must follow the reference trajectory precisely without any deviation, which is the primary focus of this thesis in alignment with the Autobike project.

1.3 Contributions

1.3.1 Hardware alterations

Our primary contributions involved hardware modifications to enhance the performance and reliability of the self-driving bikes and e-scooter including

- Steering motor mount remodelling: The original steering motor mount, made from glass, exhibited cracks that could affect long-term functionality. We redesigned the mount using Aluminium to increase durability and adjust-ability. This is discussed in the Section 3.1 .
- Cable Management and encoder protection: We addressed the issue of loose wiring that posed risks to the operation of the bikes and the e-scooter. This involved securely fastening cables using zip ties and improving the protection of the steering encoder by fabricating a protective cap. These improvements reduced the chances of cable damage and enhanced the overall safety and durability of the system. This work is detailed in the Subsection 3.1.2.

1.3.2 Simulation results and near-crash scenarios

We generated and analyzed near-crash scenarios in MATLAB for the self-driving bike. These scenarios included the bike traveling on city roads, country roads, and intersections. We analyzed the deviations from the reference trajectory and contributed to refining the bike's response in such critical situations. This is covered in the Section 4.3

1.3.3 Field test setup and execution

We setup and configured the self-driving bikes and e-scooter for field tests at Astazero discussed in the Chapter 5. This involved preparing the bikes, ensuring that

all components were functioning properly as needed to run multiple test scenarios under real-world conditions.

1.3.4 ESCON studio configuration and steering motor calibration

As part of ensuring the steering motor's efficient operation, we configured using ESCON Studio to fine-tune the motor, ensuring the steering angle to remain within operational range. The configuration process and its impact on the tests are covered in the Subsection 5.1.2.

1.3.5 Analysis of e-scooter and bike testing (outdoors and indoors)

We performed analysis of e-scooter and self-driving bikes during indoor and outdoor tests. Analyzing performance across various metrics, including steering rates, balance parameters, and comparing trajectory-following capabilities. This analysis provided insights into the bike's behavior for different tests. The results and findings are detailed in the Chapter 5.

2

Hardware Components and Softwares Used for the Self-driving Bikes

This chapter elucidates the hardware components along with the softwares used for controlling the self-driving bikes and e-scooter [7].

2.1 Platform

The bikes and the e-scooter are built to have the same platform which implies they have identical hardware components. The bicycle and e-scooter as shown in the Figure 2.1.

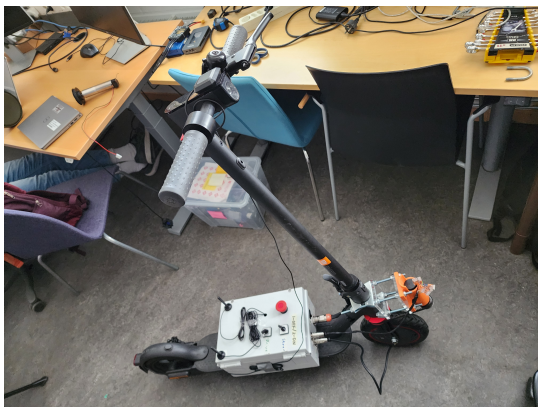

(a) E-Scooter

(b) Red bike

Figure 2.1: Autobikes used in the project

2.1.1 Hardware components inside the control box

The description and the pictures of the components inside the control box of the e-scooter and bike can be found below:

1. Emergency Stop
2. Steering motor control switch
3. Forward motor control switch
4. NI myRio: SBC with an embedded FPGA board and a microprocessor.
5. DC-DC converter

6. myRio I/O PCB
7. IMU: 3-axis accelerometer/gyroscope/magnetometer (PmodNAV LSM9DS1)
8. ZED-F9P module: GNSS receiver by U-blox..
9. Escon 50/5: Steering motor controller by Maxon
10. FSESC 6.7 PRO: Forward motor controller
11. RUT955: Bike's router

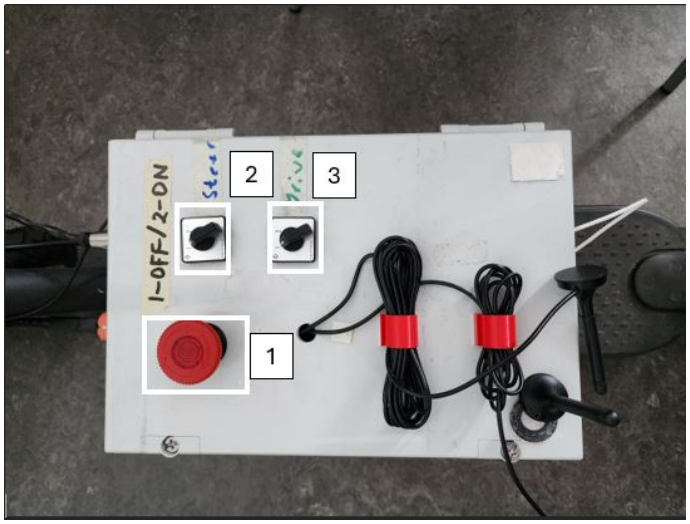

Figure 2.2: Control box which contains the hardware components of the e-scooter

(a) Hardware on one side of the control box

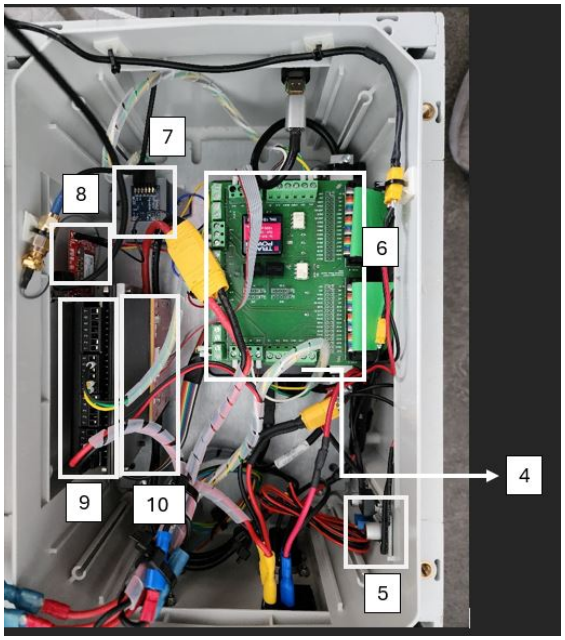

(b) Hardware components on the other side

Figure 2.3: Hardware components inside the control box

2.1.2 Hardware components outside the control box

The hardware components used are actuators such as steering motor, DCX32L by Maxon group and the in-built forward motor in case of the e-scooter and for the bikes - the Shimano Steps E6000 series. Steering motor is used to control the steering function for the bikes and e-scooter. The GPS antenna is placed outside the box to get the coordinates (latitude and longitude) of the e-scooter and bike as shown in the Figure 2.4a.

(a) GPS antenna of the e-scooter

(b) Steering motor along with the encoder on the red bike

Figure 2.4: Images of GPS antenna and steering motor with encoder

2.2 Software Tools Description

2.2.1 LabVIEW

LabVIEW (Laboratory Virtual Instrument Engineering Workbench) is a visual programming language developed by National Instruments for controlling test instruments [8]. The programming language used in LabVIEW is known as "G" and is implemented through Virtual Instruments (VI's). These blocks can range from basic mathematical functions to other VI's, referred to as sub-VI's in this context [10]. There were various sub-VI's and main VI's used for controlling different functions of the self-driving bikes.

2.2.2 MATLAB and SIMULINK

This software facilitates algorithm development, data analysis, and the creation of models and applications. MATLAB was utilised to produce near- crash scenario trajectories. SIMULINK supports continuous testing, simulation, and verification of embedded systems, and it integrates seamlessly with MATLAB, allowing the incorporation of MATLAB algorithms into models[12]. SIMULINK was used to build the bike model. This combination enables the simulation and analysis of results prior to implementing them on the hardware [13].

3

Hardware and Mechanical Modifications

This chapter comprises of hardware and mechanical modifications done on the e-scooter.

3.1 Hardware Alterations

3.1.1 Remodelling of the steering motor mount

We identified two drawbacks of the previous steering mount; Firstly the old mount is made of glass as shown in the Figure 3.1 and had visible cracks. Secondly, the motor height is not adjustable.

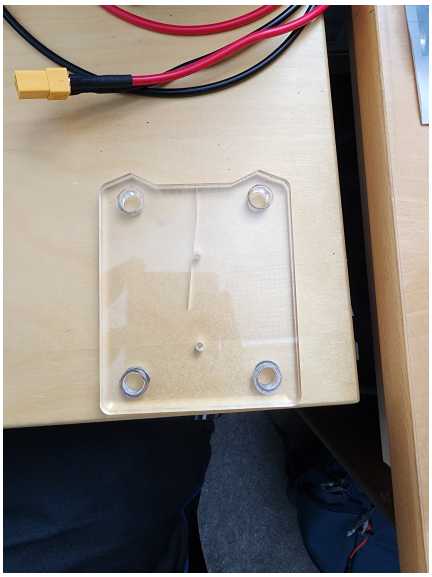

Figure 3.1: Old plate made of glass with a crack

The mount which consists of two plates were designed using the software called the Autodesk Fusion 360. The redesigned plates are made of Aluminium as they are reliable and durable. The plates have multiple holes drilled as they allow for a change in the motor height and if necessary can be moved forward or backward based on the tension required in the belt on the belt pulley system. The CAD model for the plates and the final mount setup are shown in the Figures 3.2 and 3.3 respectively.

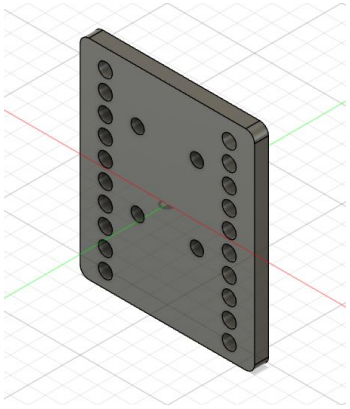

(a) CAD model of the plate

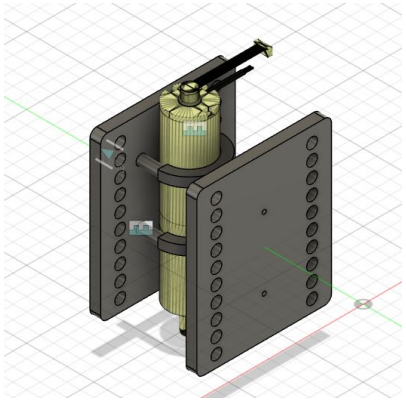

(b) Final assembly of the mount along with the motor

Figure 3.2: Images of the new mount's CAD model

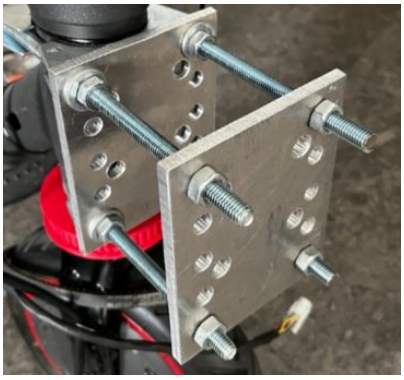

Figure 3.3: New setup with aluminium plates

3.1.2 Cable management

It was observed that loose wires posed a risk of tangling with other components. To address this, we secured the wires with zip ties to prevent any interference.

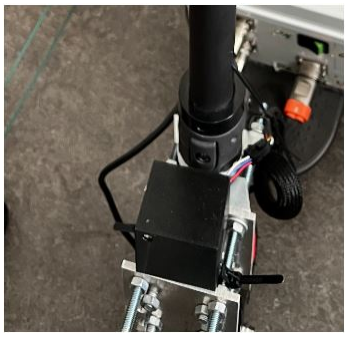

(a) Cap for encoder protection

(b) Pin header connection for steering motor encoder

Figure 3.4: Cable management on the scooter's external wires

Since the steering encoder was exposed, we designed and fabricated a protective cap. This cap is shown in the Figure 3.4a and is designed to absorb external impacts and safeguard the encoder. To ensure the new steering motor operated correctly, we soldered cables and added a heat sink to maintain the integrity of the soldered connections. This process is illustrated in the Figure 3.4b.

The e-scooter's control box was moving from its original position as it was not secured to its base. For example, this movement could cause unwanted displacement of the IMU, potentially introducing noise and resulting in erroneous steering adjustments to maintain balance. To mitigate this issue, the control box was secured using Velcro as seen in the Figure 3.5. This solution restricts movement while allowing for easy removal when transporting the e-scooter to the test track or other locations.

Figure 3.5: Control box movement restricted by using Velcro

3.2 Belt Pulley Modification

In the current setup of the steering motor, the belt pulley is faced downwards. With the redesigned mount the steering motor can be placed either upwards or downwards. A self-study was performed to evaluate the best mounted position for the motor explained in the Table 3.1

Aspect	**Configuration 1**: *Circular Inner Profile Gear*	**Configuration 2**: *Elliptical Inner Profile Gear*
Installation and fit *Refers to the gear installation and fit implies the gear's hold to the steering column.*	**Pros**: Simple to install as glue will be used with the gear. Glue is applied on the inner side of the gear and placed on the steering column. The gear will be connected using screws and tightened until snug fit. **Cons**: Glue may degrade over time and needs replacement when the gear slips.	**Pros**: Provides a secure fit on the steering column due to grooves present on the column where the gear will be placed. These grooves act as a place for the gear to hold mechanically. **Cons**: Complex to design as it requires precise mounting with respect to the grooves.

Maintenance *Refers to repair and replacement.*	**Pros**: The glue can be reapplied as they are readily available. **Cons**: The glue can lose the capacity to hold over time, leading to frequently reapplying glue.	**Pros**: Gear fit is only dependent on the gear itself. **Cons**: Possibility of fracturing at the groove point.
Steering motor placement *Refers to the motor being inverted or upright.*	**Pros**: The existing mount setup has worked during the project and has been validated practically. **Cons**: Motor pin facing down, which makes the gear connected to the pin slip down due to two main factors: gravity and the counter forces from the gear attached to the steering column. (At Astazero the motor pin was drilled for the bolt from the gear to be placed in the hole to avoid slip but the drilled portion was an indentation rather than a hole, so the issue can arise in the near future due to mechanical wear.)	**Pros**: Motor pin facing up like in the bikes implies the gear connected to the pin will be intact with gravity supporting it despite the counter forces from the gear attached to the steering column.

Table 3.1: Belt-pulley configurations

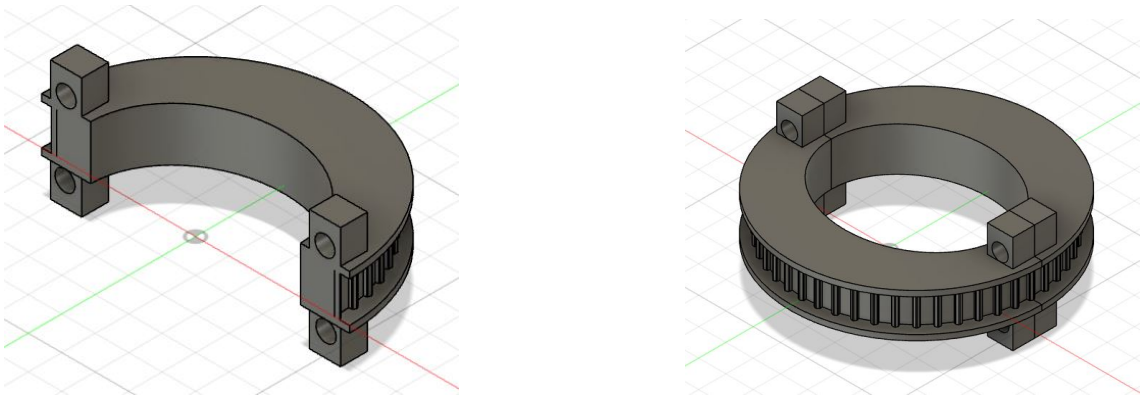

(a) Part-Elliptical gear **(b)** Final assembly-Elliptical gear

Figure 3.6: Images of the elliptical gear's CAD model

Based on the self-study, configuration 2 is the suitable option from the Table 3.1. The CAD models for the elliptical gear are illustrated in the Figure 3.6. Along with

the illustrations, the Table 3.2 lists the number of items required to build the gear. Configuration 2 allows the gear to be placed onto the steering column without the need to open it. The precise location where it should be mounted is shown in the Figure 3.3. However, the quickest way to use the steering function of the e-scooter was to use configuration 1 and it worked by adding glue to avoid slip.

Component	Quantity
Half-Gears	2
M6 bolts	4
M6 lock nuts	4

Table 3.2: List of components and their quantities for the elliptical gear

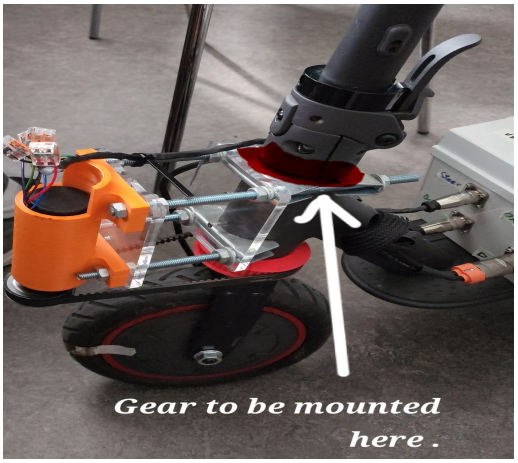

Table 3.3: Location for the elliptical gear

3.3 Alterations for Tests Indoors

The bikes and the e-scooter are tested indoors to check for balancing. When testing it indoors, the bike or the scooter is placed on the roller shown in the Figure 3.7.

Figure 3.7: Elite quick motion floating roller [15]

The e-scooter's wheelbase is small in comparison to the bike's wheelbase shown in the Figure 3.8. Therefore, a support roller is added to hold the e-scooter's rear wheel on the blue mark shown in the Figure 3.9.

Figure 3.8: Scooter on the roller

Figure 3.9: Addition of roller support on the blue mark

The support roller was designed using Autodesk Fusion 360. The pictures of the CAD models for the support roller are shown in the Figures 3.10, 3.11, and 3.15 along with the Table 3.4 elucidating the number of parts required to build the support roller.

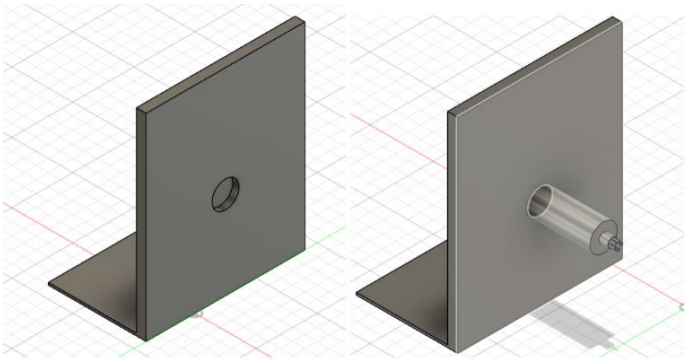

Figure 3.10: Side supports for the support roller

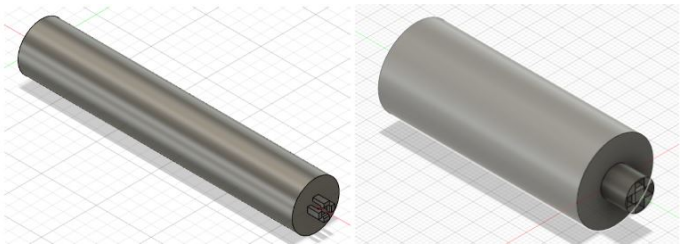

Figure 3.11: Inner and end shafts for the support roller

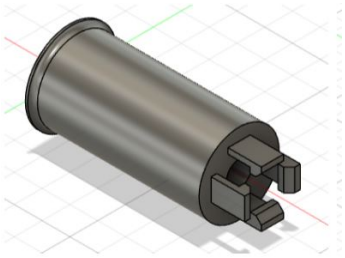

Figure 3.12: Outer cylinder for the support roller

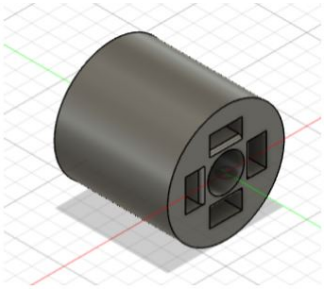

Figure 3.13: Outer cylinder connector for the roller

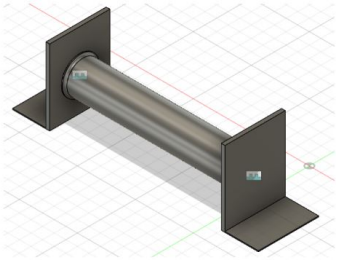

Figure 3.14: Final support roller assembly

Figure 3.15: Components of the roller along with the final assembly

Component	Quantity
Side supports	1 (Each)
Inner shaft	2
End shaft	1
Cylinder	2
Bearings (Model: 608 RS)	2
Connector	1

Table 3.4: List of components and their quantities for the support roller

The final fabrication of the support roller was done using Prusa Slicer for 3D printing all the components seen in the Table 3.4 except for the bearings. The pictures of the 3D printed components are shown in the Figures 3.16, 3.17, and 3.19.

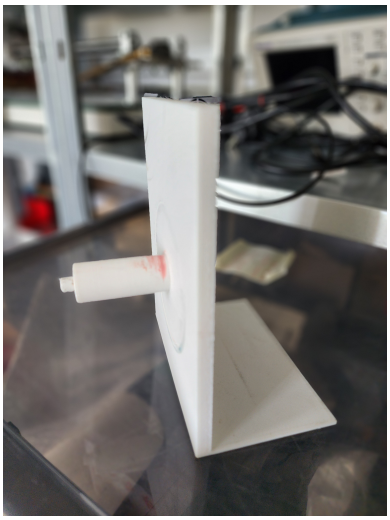

(a) Side support

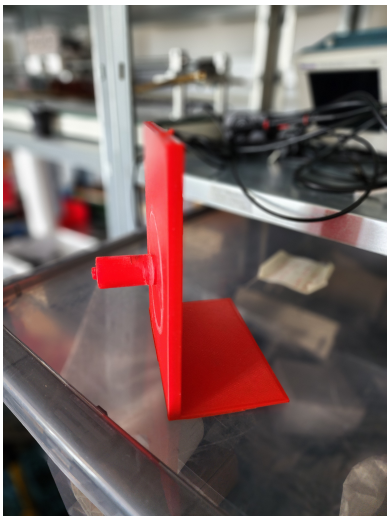

(b) Side support with inner end shaft

Figure 3.16: Side supports with end shafts

Figure 3.17: Inner shaft

Figure 3.18: Groove ball bearings [16]

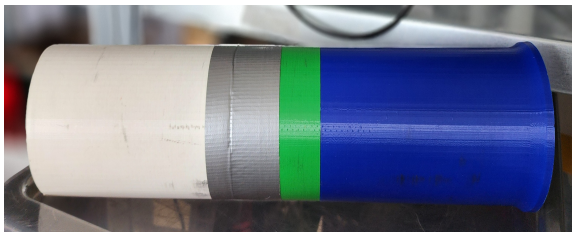

Figure 3.19: Outer cylinder and the connector

The e-scooter is placed on the support roller shown in the Figure 3.21.

Figure 3.20: Final 3D printed support roller

Figure 3.21: E-Scooter placed over the roller

Testing with the support roller, observations were made leading to the conclusion that snap fits are a bad solution as the fits became worn due to friction generated between the plastic 3D prints resulting in loosening of the connection between the

cylinder and the connector. Therefore, as a temporary solution, scotch tape was used to hold the connector and outer cylinder as shown in the Figure 3.19. To solve the problem without using scotch tape, instead of having a connector in between two outer cylinders, which were connected with the help of snaps, the whole outer cylinder was 3D printed as shown in the Figure 3.22.

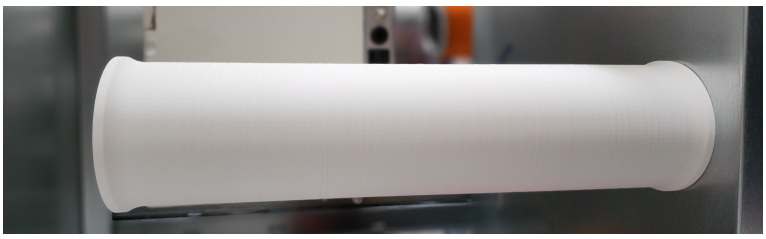

Figure 3.22: New outer cylinder for the support roller

The snap fit issue was resolved, friction was still a concern. The friction was generating between the cylinder and the inner shaft, which hindered the continuous movement of the support roller. This friction was due to plastic-on-plastic contact between the cylinder and the inner shaft. To eliminate the issue, the number of ball bearings were increased and a metallic inner shaft was introduced. Instead of using two ball bearings, we used five bearings placed optimally and secured on the metal shaft with nuts to keep them in place, as illustrated in the Figure 3.23. This arrangement reduced the friction between the cylinder and the inner shaft.

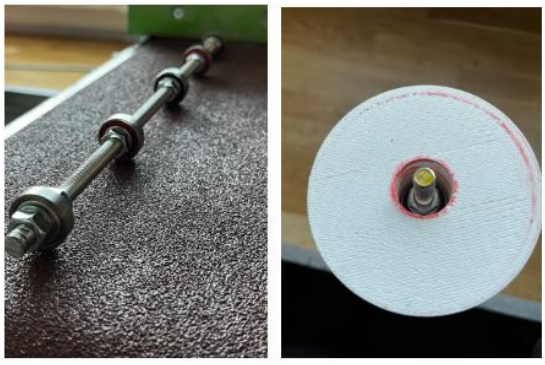

Figure 3.23: Inner metal shaft and five ball bearings

Figure 3.24: Use of aluminium tape on the side supports

To reduce the friction between the cylinder ends and the side-support, aluminum tape was used, as shown in the Figure 3.24. This ensured that the contact between the cylinder ends and the side-supports did not generate friction, allowing the roller to move freely.

3.4 Altering the Center of Mass

The e-scooter's Center of Mass (CoM) is simplified and divided into four parts as shown in the Figure 3.25,

- **Base**: Comprising the battery, frame, and forks, modeled as a homogeneous box, with its CoM at the center of its length and height.
- **Wheels**: Front and rear wheels have their CoM located at their centers and are considered along with the base.
- **Steering Bar**: Modeled as a homogeneous cylinder.
- **Handlebar**: Modeled as a homogeneous cylinder.

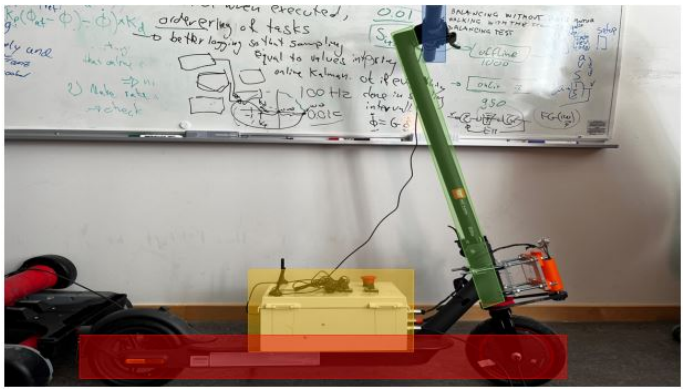

Figure 3.25: Representation of the CoM division in the e-scooter [14]

To improve the balance of the e-scooter, an additional weight of 1.35 kg was added. Velcro was attached to the steering bar, and a harness was used to secure the weights in place, as shown in the Figure 3.26. Increasing the CoM by adding weight to the steering bar raises the e-scooter's sensitivity to roll. This increase in sensitivity allows for more predictable and controllable roll behavior, which is beneficial for stability during maneuvers [17].

Figure 3.26: Adjustable weight to alter CoM

4

Simulations Performed on the Bikes and the E-scooter

This chapter presents simulations to assess the ability of the bikes and the e-scooter to follow reference trajectories with minimal oscillations and to evaluate the balancing control of the e-scooter by tuning the proportional (Kp) and derivative (Kd) gains. Additionally, near-crash scenarios involving car-bike interactions are explored to improve safety systems in AD/ADAS.

4.1 Path Deviation from the Reference Trajectory

There is a drift from the reference path when tested for repeatability of the trajectory as seen in the 8-trajectory's bird view in the Figure 4.1, it can be observed that the true trajectory of the bike represented by the orange line moves away form the reference trajectory over a period of time represented by the blue line.

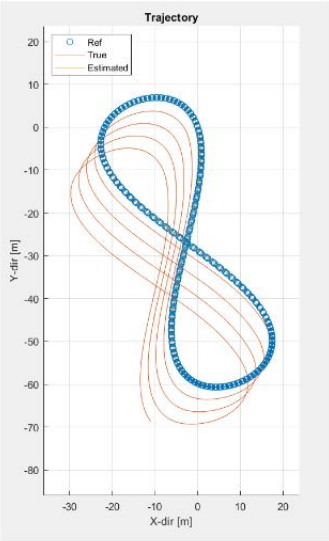

Figure 4.1: Drifting of self-driving bike from the reference trajectory

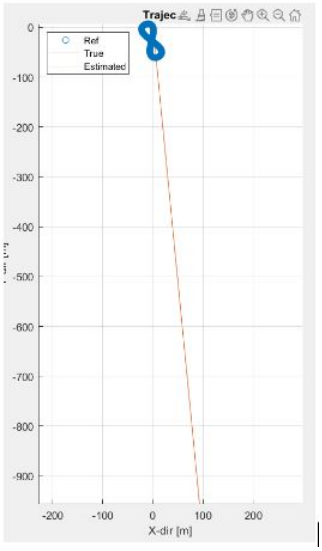

Figure 4.2: Parameters set as follows indoorTuning = 0 and the badGPS = 1

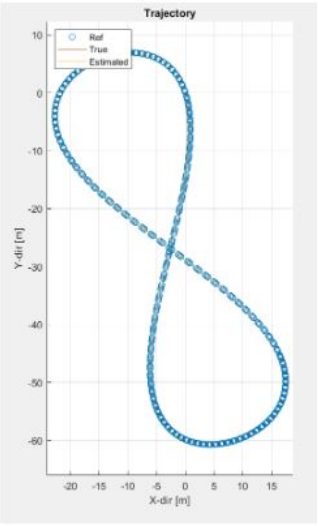

Figure 4.3: Parameters set as follows indoorTuning = 0 and the badGPS = 0

This drift could be due to the fact that the model cannot differentiate if the test is performed indoors or outdoors. When the test is being performed indoors, the GPS signal tends to be calibrated improperly. The following tests were conducted to find the cause of drifting:

- Two parameters were used in the MATLAB file for the bikes and the e-scooter which are for GPS signals indoors and outdoors.
  - badGPS = 0
  - indoorTuning = 0

  when these parameters were set to zero, there was no drifting.
- When the indoorTuning = 1 and the badGPS = 1, the bike is being tested indoors which leads to GPS signal blockage and the bike goes off the path causing drift.
- The badGPS parameter is used to make the signal steady from the beginning of the simulation. When the indoorTuning = 0 and the badGPS = 1, the GPS signal which is the X and the Y coordinates pauses after 1 second and cannot follow the trajectory as seen in the Figure 4.2.

4.2 Balance Parameters Investigation for the E-scooter

The balancing parameters of the e-scooter which are the proportional (Kp) and the derivative (Kd) gains have been implemented based on an iterative approach. The simulations were performed initially with Kp=0 and Kd=4 with the results shown in the Figure 4.4.

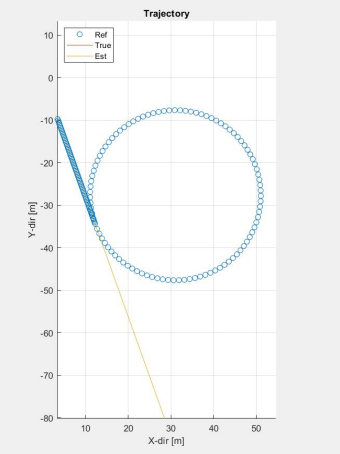

Figure 4.4: When Kp=0 and Kd=4 is set as the parameters of the balancing controller, it can be seen that the e-scooter is unable to follow the reference trajectory, therefore, further tuning of the parameters were performed

As we had initialized the Kp as zero, the e-scooter was not responsive to the set of gains given to the balancing controller and was not able to follow the trajectory properly. To overcome this issue, Kp was to set to 0.5, to check if the e-scooter

responds to this value of the gain. It was observed that the e-scooter responds and tries to follow the trajectory but, there were large oscillations as seen in the Figure 4.5a.

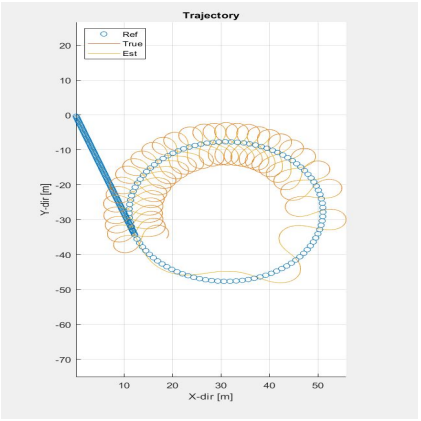

(a) Kp=0.5 and Kd=4

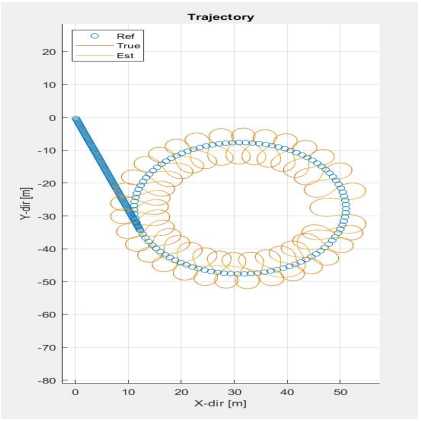

(b) Kp=0.5 and Kd=3.5

Figure 4.5: Simulation with same Kp and different Kd

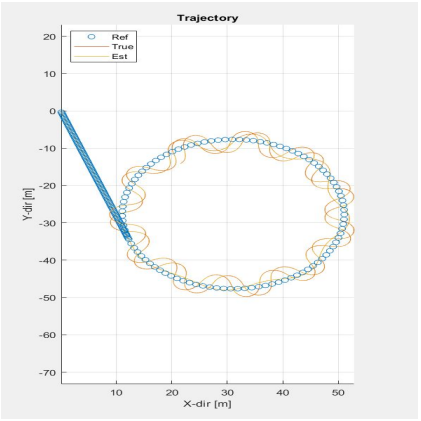

(a) For Kp=0.5 and Kd=3,the e-scooter is following the reference trajectory but has oscillations

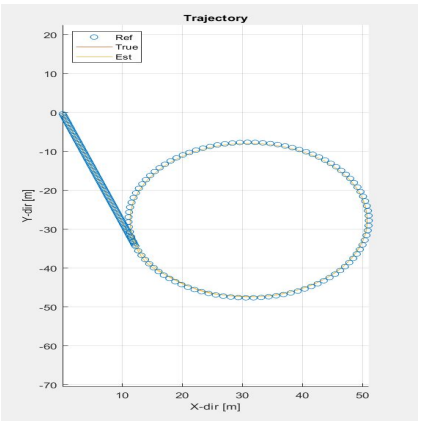

(b) For Kp=1 and Kd=3, the e-scooter is able to follow the reference trajectory

Figure 4.6: Simulation with same Kd and different Kp

To reduce large oscillations Kd was reduced from 4 to 3.5 which resulted in the oscillations being persistent but the frequency of these oscillations were better than before as seen in the Figure 4.5b. The frequency of the oscillations is bad as the e-scooter has to follow the reference trajectory without oscillations. We fine tuned the balancing controller with the values Kp=0.5 and Kd=3 and noticed oscillations. To further reduce the oscillations seen in the Figure 4.6a, the Kp was set to 1 and Kd to be 3. The Figure 4.6b shows there are no oscillations and the e-scooter is able

to follow the reference trajectory properly. Therefore, the final parameters for the balancing controller of the e-scooter are ***Kp=1*** and ***Kd=3***.

To validate the e-scooter balancing, the analysis of roll is crucial and the plots can be seen in the Figure 4.7, as they provide insight into the extent of roll when attempting to follow the reference trajectory. Smaller amplitude and lower frequency oscillations indicate that the e-scooter is likely to follow the reference trajectory, with minimal deviations. A lower oscillation rate signifies that the e-scooter is effectively tracking the reference trajectory with minimal deviation. This is essential for stability and control, as reduced roll angles correspond to smoother and accurate path following. Furthermore, the steering angle is directly influenced by the amount of roll experienced by the e-scooter. When the roll increases, the e-scooter must adjust its steering angle to counteract the roll and maintain balance. The ability to control the roll through steering adjustments is a key factor in achieving a balanced and stable ride.

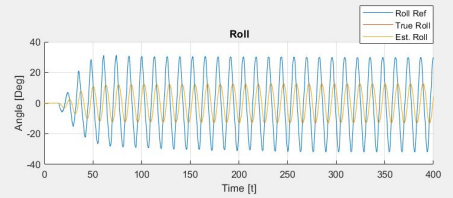

(a) Kp=0, Kd=4

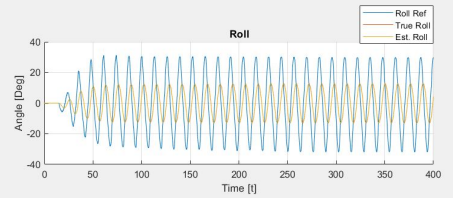

(b) Kp=0.5, Kd=4

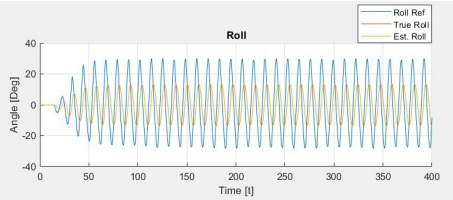

(c) Kp=0.5, Kd=3.5

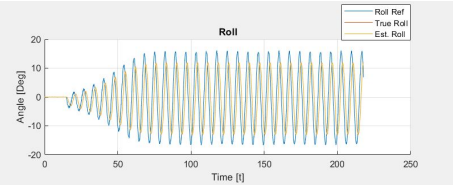

(d) Kp=0.5, Kd=3

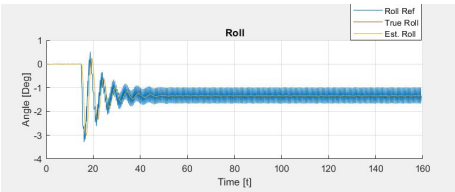

(e) Kp=1, Kd=3

Figure 4.7: Respective roll plots for the trajectories in the Figures 4.4, 4.5, and 4.6

4.3 Near-Crash Scenarios

Near-crash scenarios are of vital importance when examining interactions between cars and bikes due to their potential for severe consequences and their critical role

in enhancing safety systems. These scenarios typically arise in situations where cars and bikes come dangerously close to each other, narrowly avoiding a collision [18]. The influence of near-crash scenarios on AD/ADAS technologies is profound. These systems might benefit on using extensive datasets to refine their algorithms, which improve vehicle safety and decision making processes. For instance, understanding the conditions that lead to near-crashes can enhance the effectiveness of collision avoidance systems, adaptive cruise control, and automatic emergency braking. Integrating near-crash scenarios into the development of these technologies enables manufacturers to build more responsive and intelligent systems that better anticipate and respond to potential dangers involving cyclists, thereby improving overall road safety and decreasing the likelihood of actual collisions [19]. Thus, we have developed trajectories in MATLAB for Volvo cars. In the Subsections 4.3.1, 4.3.2, and 4.3.3 three trajectories have been discussed. There is a delay in the true and estimated roll signals compared to reference roll signals which can occur due to actuator dynamics (actuators take time to respond) and sensor delays (signal propagation time).

4.3.1 Bike travelling on city roads

This scenario involves the bike travelling on the city roads. In these roads, the bike tends to travel in low speeds due to traffic conditions. We have considered an example of bike travelling in a parking lot along with the car reversing to have an interaction between car and bike. These conditions provide the bike to wiggle with very less amplitude given as 0.5 for analysis in MATLAB and the bike is travelling in a straight line as seen in the Figure 4.8.

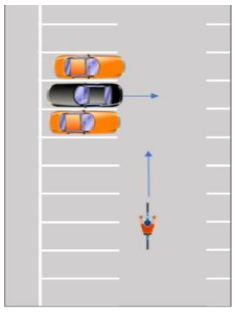

(a) Bike passing behind reversing vehicle

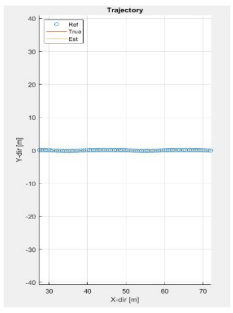

(b) Trajectory of the bike

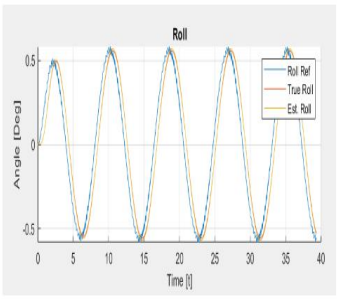

(c) Roll of the bike while following the trajectory in the Figure 4.8b

Figure 4.8: Bike travelling in a parking lot

4.3.2 Bike travelling on country roads

When the bike is on a country road without designated bike lanes and encounters strong winds along with the pedaling of the bike, a significant wobbling of the bike is observed. The trajectory reflects this scenario, with the bike being overtaken by a car while also facing an oncoming vehicle, as illustrated in the Figure 4.9.

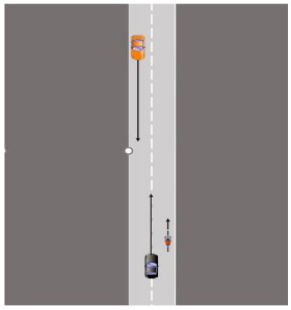

(a) Car overtaking the bike

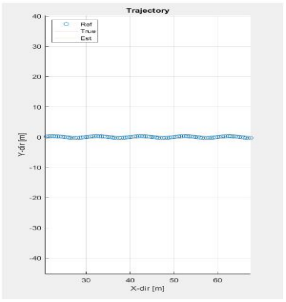

(b) Trajectory of the bike

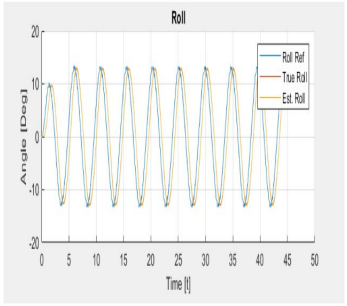

(c) Roll of the bike while following the trajectory in the Figure 4.9b

Figure 4.9: Bike travelling on a country road

4.3.3 Bike taking a turn at the intersection

This scenario is set up at an intersection where the bike travels at a constant speed of 2.4 m/s, making a turn with a turning radius of 14 meters, while the car proceeds in a straight path, as shown in the Figure 4.10. The scenario illustrated in the Figure 4.10a is created to represent the bike's trajectory to understand the car's active safety function's behavior as there is a possibility of generation of a false positive signal, either by warning the driver to brake or activating the AEB. Both of the outcomes are unnecessary as the paths do not intersect.

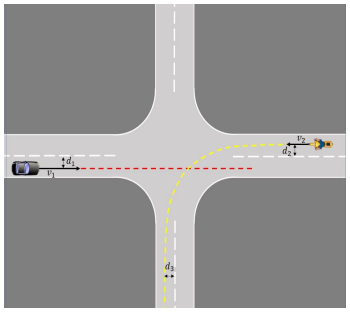

(a) Car and Bike's path at an intersection

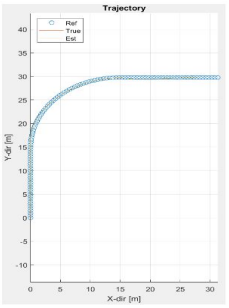

(b) Trajectory of the bike

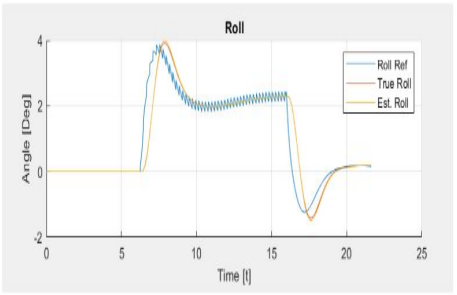

(c) Roll of the bike while following the trajectory in the Figure 4.10b

Figure 4.10: Bike turning right in an intersection and car following a straight path

5

Analysis of E-scooter and Bikes Tested Outdoors and Indoors

5.1 Analysis of E-scooter Tests

5.1.1 E-scooter tests with the old motor

The initial steering motor which is referred to as the old motor used was SD3039, 12 V, spur-gear DC motor from Transmotec with an encoder. The new steering motor used is DCX32L 24 V with the steering sensor, ENX10 EASY 500IMP. The maximum velocity is 30000RPM and a maximum resolution of 1024 counts per revolution. The encoder is mounted on the steering motor to measure the steering angle which further transmits the measurements to the myRIO which is the same as the one's present on the bikes. The e-scooter was tested to check for balance. The tests done indoor on the roller can be seen in the plots shown in the Figure 5.1.

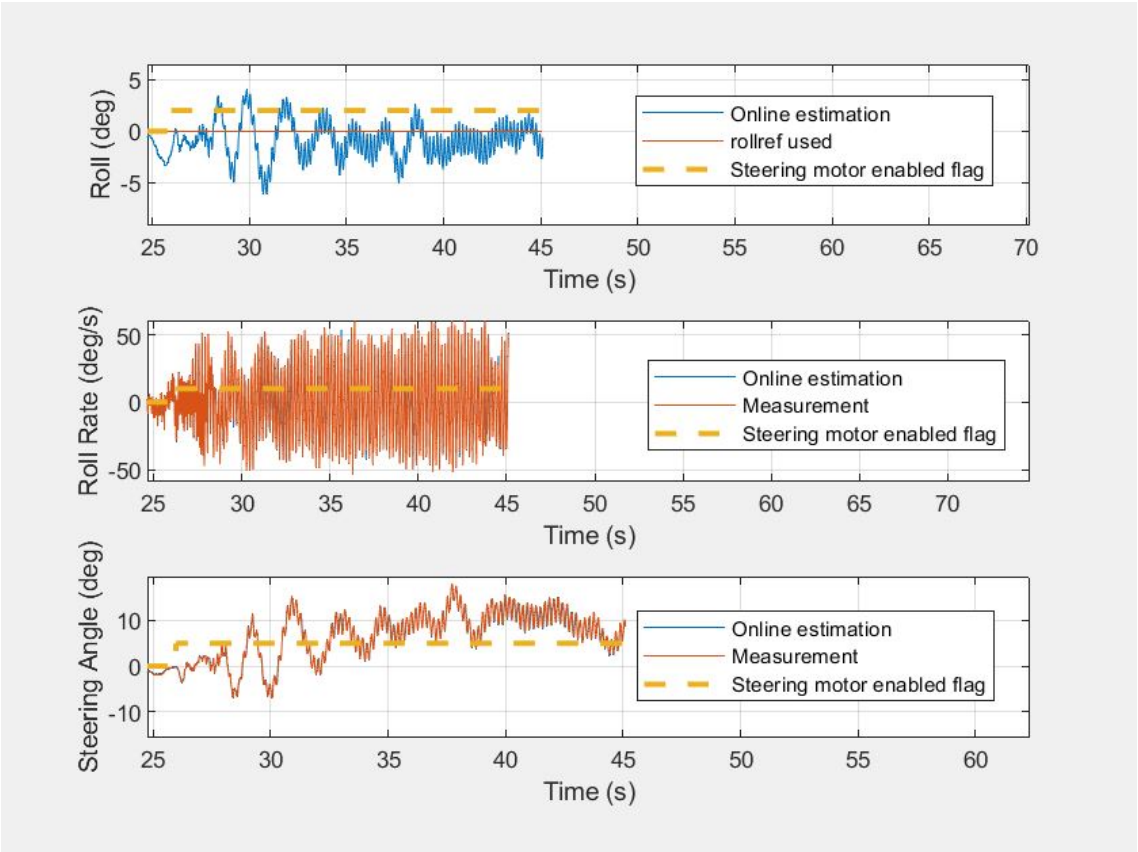

Figure 5.1: E-scooter test on the roller with motor SD3039

All the three plots show minor fluctuations which can be induced by the 3D printed roller's surface causing the e-scooter to slightly bounce up and down. The plot at the top shows the roll in degrees vs time and indicates the scooter is rolling on both sides approximately between 3 to -5 degrees over a period of time and the online estimation matches the reference roll used. The roll rate vs time plot indicates the rate of change of roll and the online estimation is consistent with the measurement. The steering angle vs time plot is consistent with roll vs time plot indicating that the scooter is trying to balance. Many tests were conducted on the roller but they were inconsistent as the roller constantly had to be improvised and repaired. The plot shown in the Figure 5.1 is one of the best results obtained as the e-scooter tries to balance as seen from the plots and it lasted for approximately 18 seconds.

The e-scooter was tested outside in the football field and the Chalmers parking lot. The plots in the Figure 5.2 is for the scooter balancing test conducted in the football field.

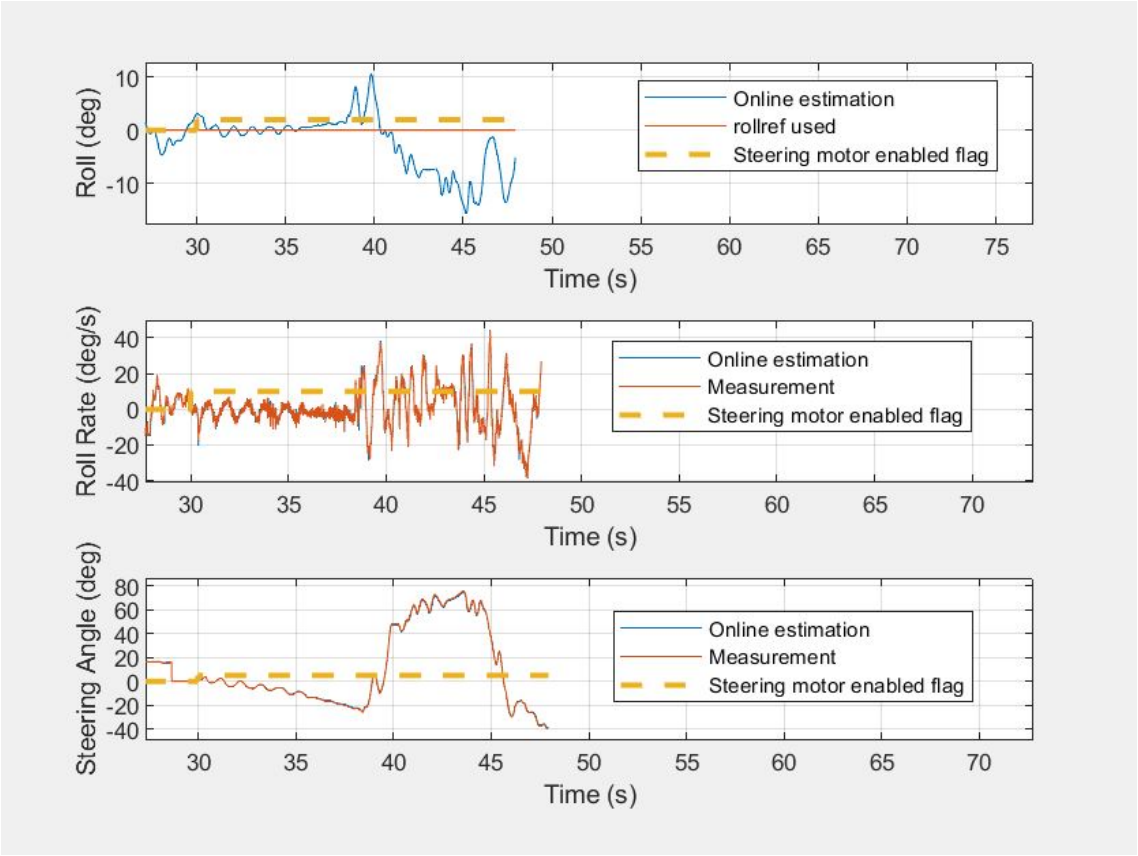

Figure 5.2: E-scooter tested outdoors in the football field with motor SD3039

The top plot in the Figure 5.2 shows roll in degrees vs time which indicates that the e-scooter starts rolling on one side around 10 degrees and gradually starts tilting to the other side and the steering for the roll can be observed in the bottom plot where it is consistent with the roll as indicated in the top plot. The roll rate vs time and the steering angle vs time plots indicate the online estimation is consistent with the measurement. The e-scooter balanced for about 17 seconds.

Balancing tests were conducted in Astazero for the e-scooter and it was observed that there was an issue with the steering motor.

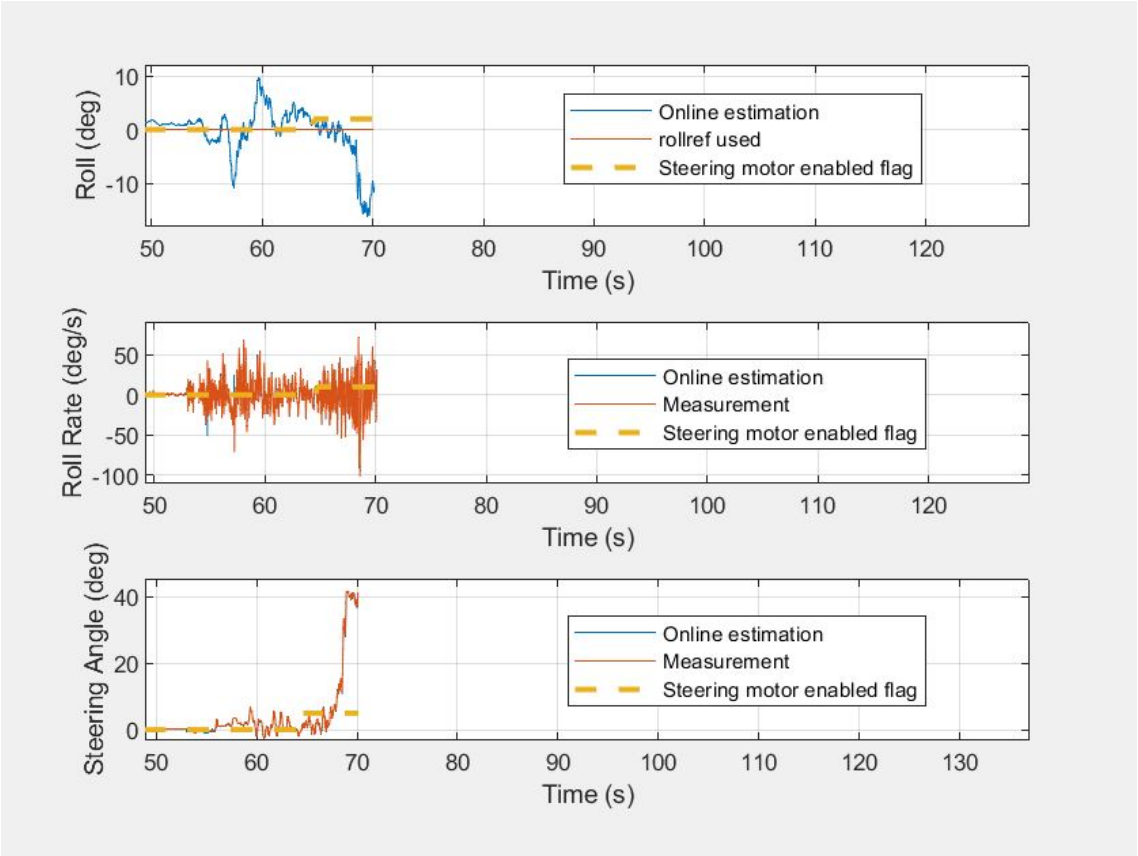

Figure 5.3: E-Scooter's steering issue

The e-scooter was tested to balance on the roller and the steering motor behavior observed was not ideal as seen in the plots shwon in the Figure 5.3 of this test. The steering angle reaches around 40 degrees and does not return although the steering angle limit set was between ± 1.5 radians or 86 degrees.

5.1.2 Steering motor replacement

To understand the behaviour of the steering motor at Astazero, it was observed that the belt pulley of the motor was slipping down due to the motor mount position. To solve the issue a hole was drilled in the shaft to hold the belt pulley in position which in turn ensures the gear doesn't slip. The e-scooter was tested after the modifications were made, there was no improvement as the Steering encoder position was null with no value. Therefore, we tried re-configuring the motor. Since, it was not part of maxon group, the software showed unusual errors due to which the motor was not re-configurable.

This series of failures led to the replacement of old steering motor which is the same used in the bikes and is a part of maxon group.

Figure 5.4: New steering motor for the e-scooter

The new steering motor shown in the Figure 5.4 was configured using Escon studio after the steering motor angles initially showing values in the range of thousands of degrees as shown in the Figure 5.5.

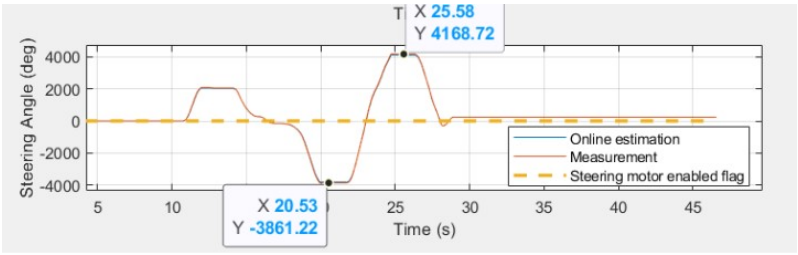

(a) New steering motor before configuring

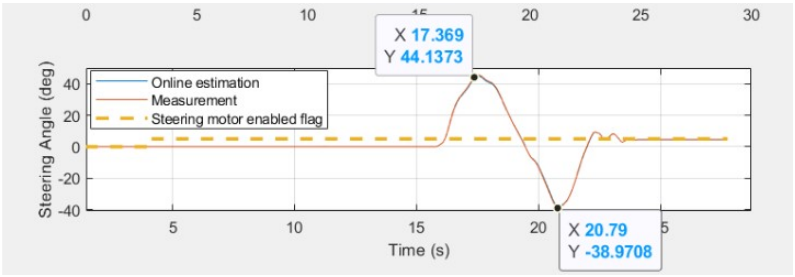

+

(b) New steering motor after configuring

Figure 5.5: Comparison of the new steering motor before and after configuring

5.1.3 E-scooter tests with the new motor

- The steering angle was set in the right range and the motor was successfully configured, the new motor was mounted and balancing tests were conducted. The set of plots as shown in the Figure 5.6 indicate the responsiveness of the steering motor. This set of plots show that the motor's steering angle is consistent with the change in roll and visually the responsiveness seemed adequate.

- The scooter was tested indoors on the roller. It can be seen from the plots shown in the Figure 5.7 that the e-scooter is unable to balance as confirmed by the Roll vs time and Steering angle vs time plots. After facing the same result by conducting tests on the roller, we moved outdoors to perform balancing tests.

- The plots shown in the Figure 5.8 are for the balancing tests conducted outdoors in the Chalmers parking lot. The steering angle vs time plot shows that the e-scooter moved in one direction for about 13 seconds and started steering in the other direction and eventually stopped. In the test the e-scooter tried to balance for approximately 8 seconds.

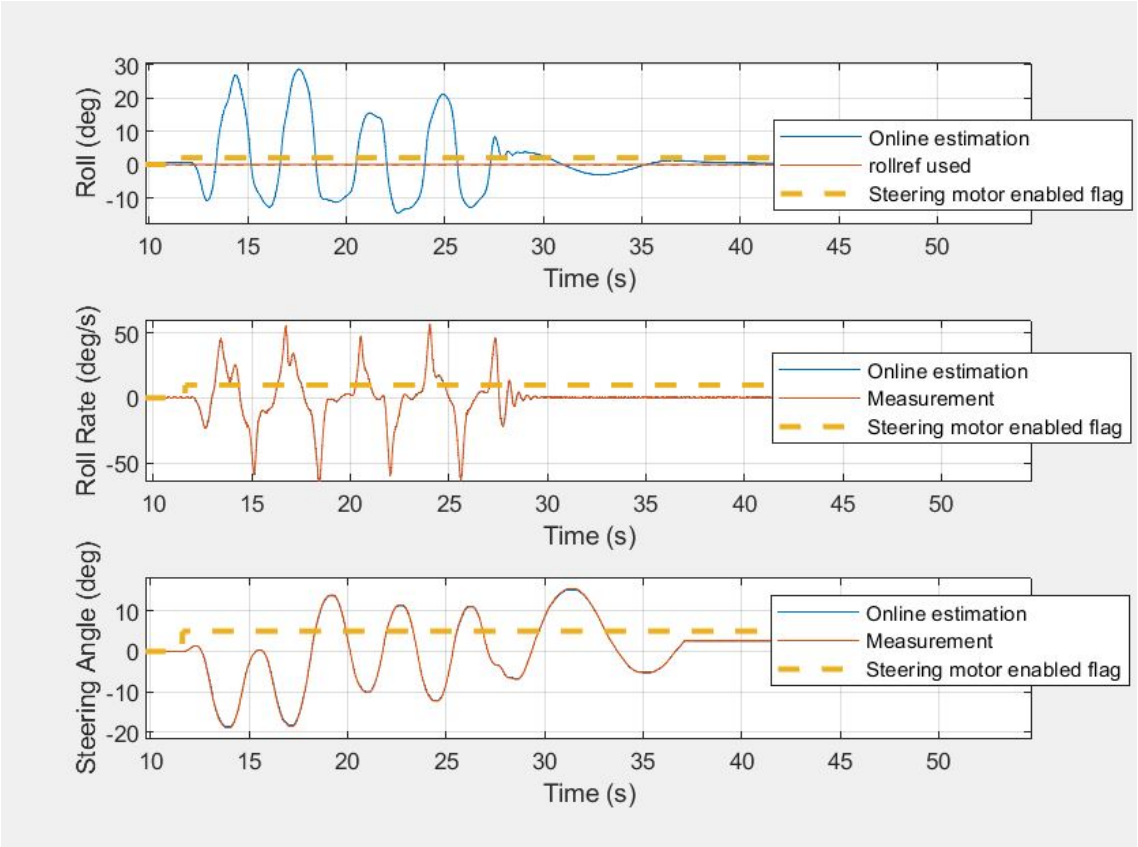

Figure 5.6: Testing with the new steering motor in air (front wheel) to check for steering responsiveness

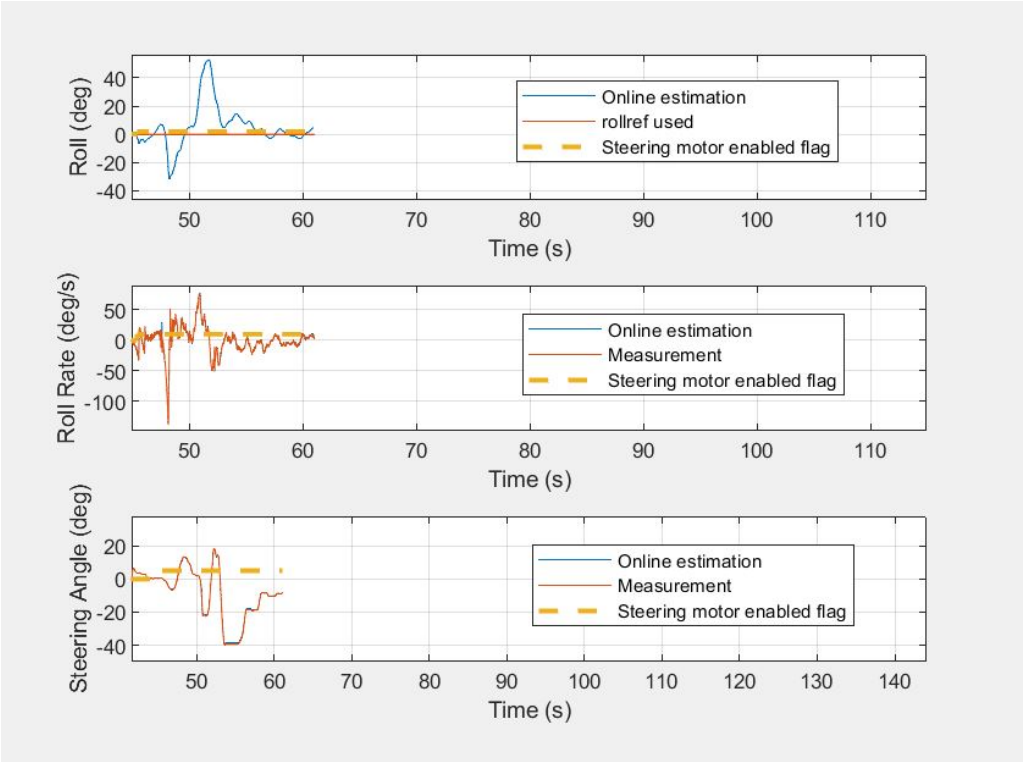

Figure 5.7: Testing with the new steering motor on the roller

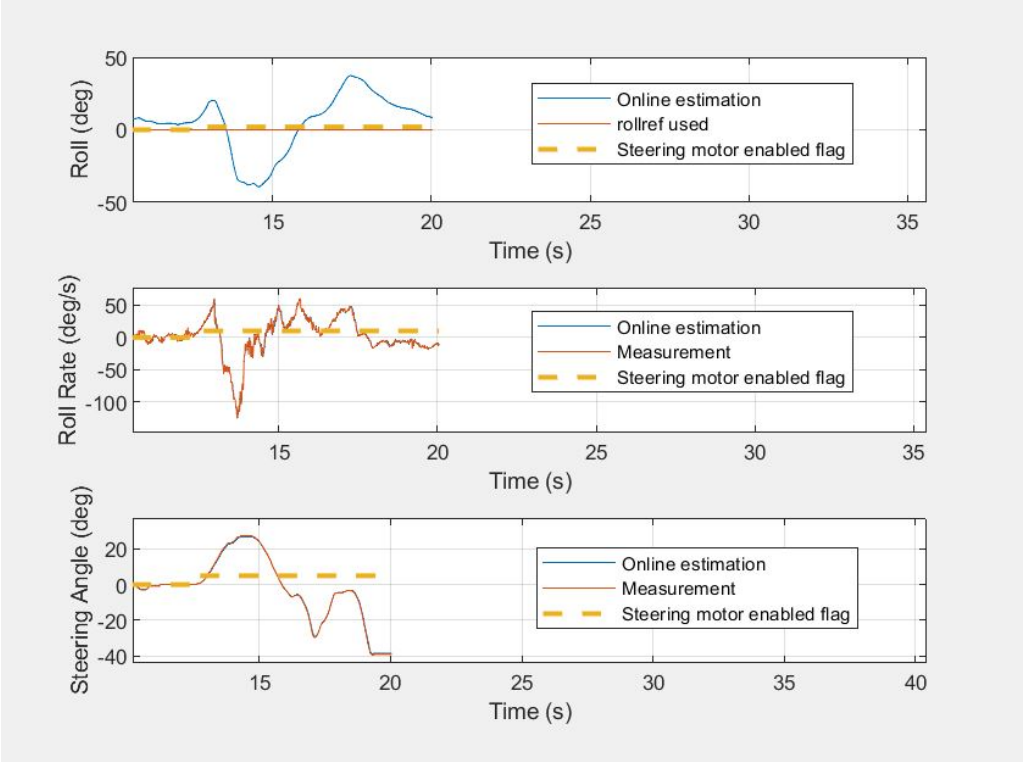

Figure 5.8: Testing with the new steering motor outdoors at Chalmers parking lot

5.2 Analysis of Plastic Bike Balancing at Astazero

The plastic bike is a bike built by students from 3D printed parts and plastic tubes as it can be replaced after a destructive test. The green bike and the plastic bike share the same control box and drive motor which is attached in the wheel.

Figure 5.9: Testing of plastic Bike for balancing at Astazero

The plastic bike was tested for balancing at Astazero. The Figure 5.10 shows plots for Roll angle, Roll rate, and Steering vs time which are required to analyse and check if the plastic bike can balance.

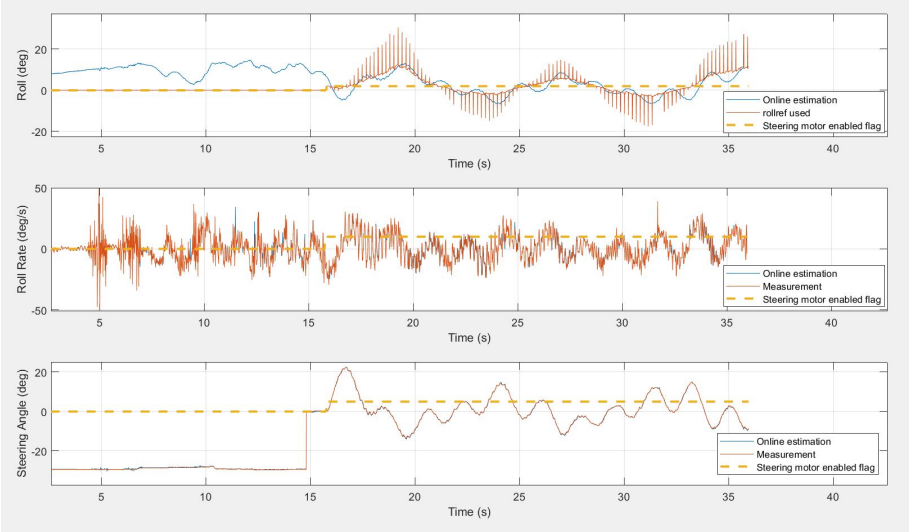

Figure 5.10: Plots for balance analysis on the plastic bike

- Roll vs time: The plot indicates how much the bike rolling in degrees. The oscillations indicate the bike was unable to stabilize laterally. As a stable bike would have minimal fluctuations although there can be roll.
- Roll rate vs time: The roll rate or the angular velocity is the rate of change of roll expressed in degrees per second. The plot shows roll rate oscillating with high frequency and amplitudes ranging in between ±40 deg/s which indicates the bike is rapidly rolling in either direction indicating instability.
- Steering angle vs time: The plot indicates how much the front wheel is turning left or right in degrees and how fast. Around 16 seconds when the steering is enabled it can be seen that the bike is steering to counter the roll but the curves are not smooth as they have fluctuations. From the three plots it is observed that the bike balances but wiggles.

5.3 Analysis of Test Results Performed at Astazero for the Same Trajectory on Different Bikes

The red bike and the green bike were fed with the same trajectory and uploaded in their respective myrio's. Ideally both the bikes should behave the same way but the following was observed: The green bike is experiencing significant oscillations across different metrics as compared to the red bike. The comparisons of the trajectories can be seen in the the Figure 5.11.

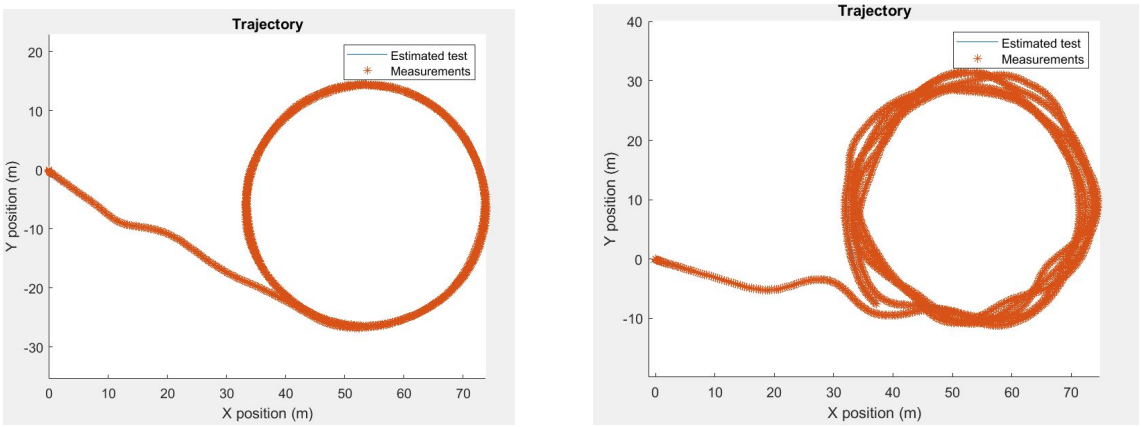

(a) Red bike trajectory

(b) Green bike trajectory

Figure 5.11: Bike trajectories

Here is the comparison for other metrics which indicate the oscillations occurring in the green bike.

- Steering rate: The steering rate plots as seen in the Figures 5.12 shows oscillations in the range of ±0.6 rad/s for the red bike and ±2.5 rad/s for the green bike. There is noise present in the red bike but not as severe as the green bike which indicates that the red bike is more stable.

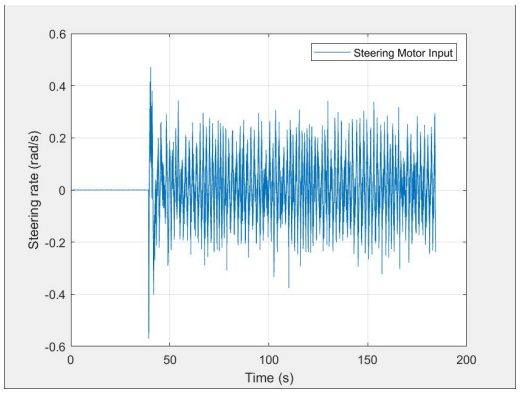

(a) steering rate for the red bike

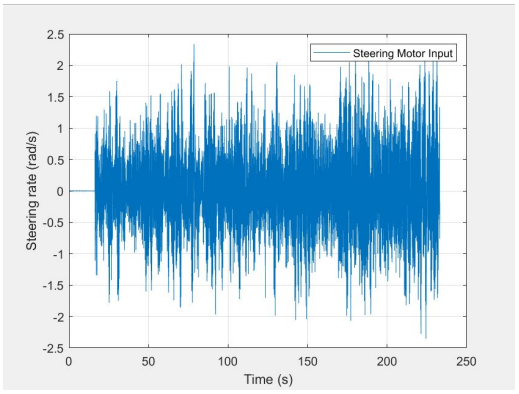

(b) steering rate for the green bike

Figure 5.12: Steering rate for the bikes

- Lateral & Heading errors: The plots shown in the Figures 5.13 are for the lateral and heading errors vs time respectfully. Lateral error oscillates at a higher range of ± 4 meters for the green bike as compared to the red bike which has lateral error oscillations in the range of ± 2 meters which indicates persistent instability for the green bike to maintain its trajectory. Heading error for the red bike is minimal and settles over time whereas for the green bike it oscillates between ± 40 degrees which indicates the green bike is struggling to maintain a stable heading.

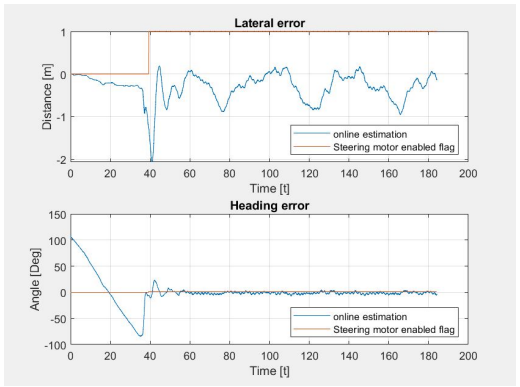

(a) Lateral & heading error red bike

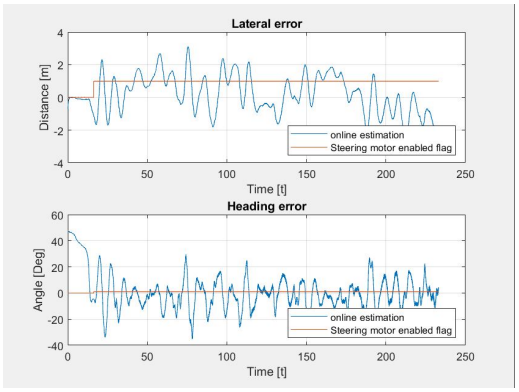

(b) Lateral & heading error green bike

Figure 5.13: Lateral & heading errors for the bikes

- Forward motor current: The plots shown in the Figures 5.14 indicates that the red bike is working better as compared to the green bike. For the green bike the motor current fluctuates with respect to the input current given which implies that the green bike is continually trying to correct but is unable to find a stable state.

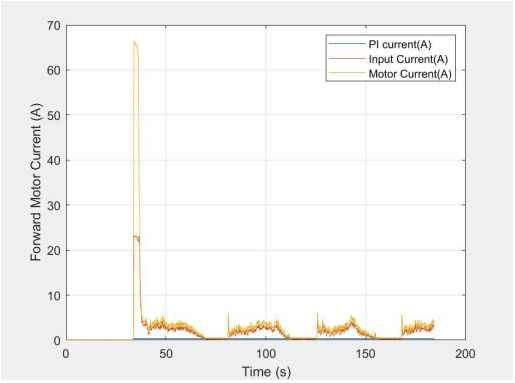

(a) Forward motor current red bike

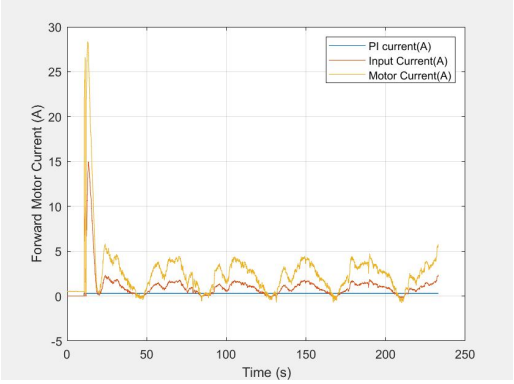

(b) Forward motor current green bike

Figure 5.14: Forward motor current for the bikes

- Delta reference and roll reference: The Delta_ref and the Roll_ref shown in the Figures 5.15 initially oscillate for the red bike but then stabilize to consistent values finding a steady state as compared to the green bike which has oscillations that do not stabilize.

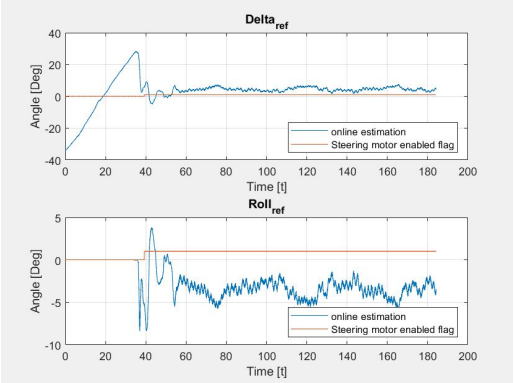

(a) Delta reference and roll reference red bike

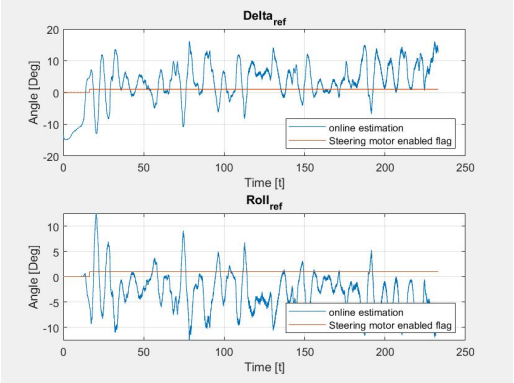

(b) Delta reference and roll reference green bike

Figure 5.15: Delta reference and roll reference for the bikes

- Error contributions: The plots shown in the Figures 5.16 are the error contributions. The red bike error contributions settle and reach more consistent values. For the green bike it can be seen that lateral and heading error contributions have significant oscillations throughout the time period. Dpsiref contribution remains erratic which implies that the desired steering rate is being continually adjusted without reaching a steady state.

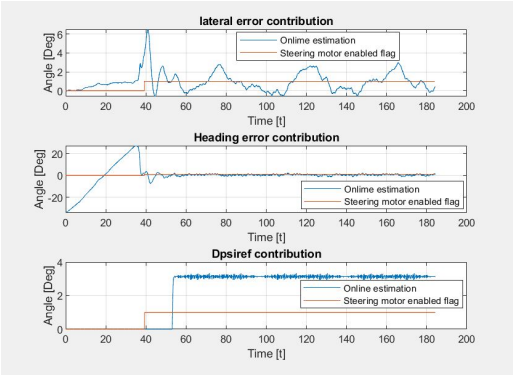

(a) Error contributions the on red bike

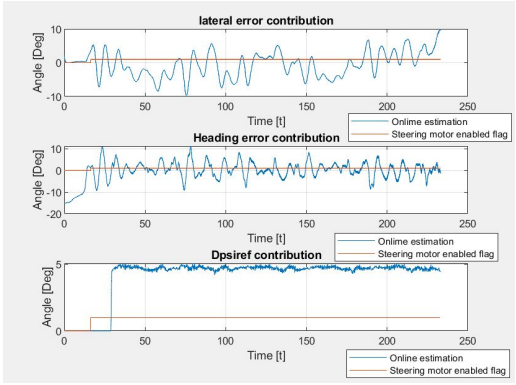

(b) Error contributions on the green bike

Figure 5.16: Error contributions of the bikes

- Positions and heading vs time: The plots shown in the Figures 5.17 are for the position vs time and heading vs time for the bikes. The red bike X and Y position curves are smoother, and the degree of deviation is less compared to the green bike. The heading for the red bike does not show any fluctuations over time, as opposed to the green bike, which exhibits noise.

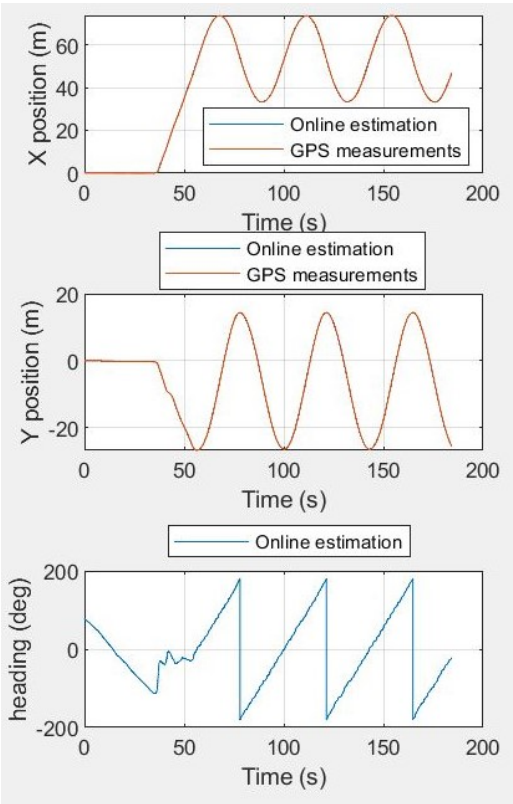

(a) Positions and heading vs time for red bike

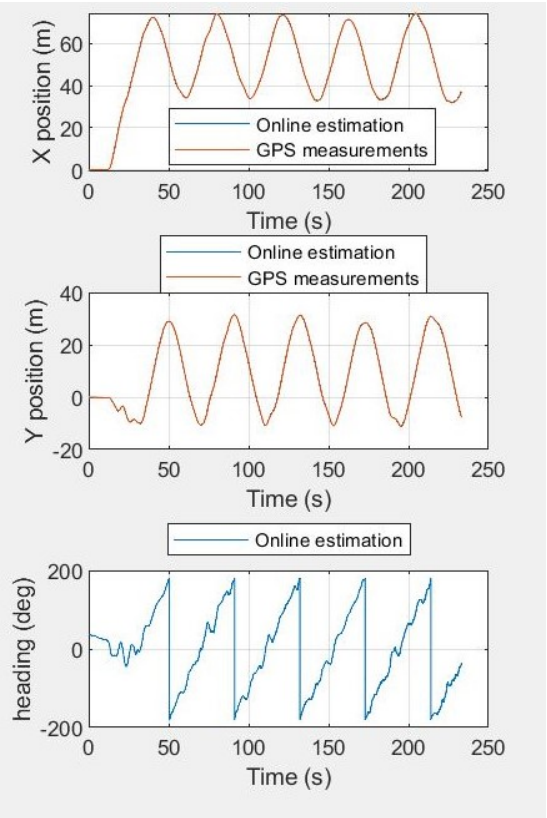

(b) Positions and heading vs time for green bike

Figure 5.17: Positions vs time and heading vs time of the bikes

- Roll and roll rate vs time:
  - Roll vs time: The top plots in the Figures 5.18 are the roll vs time plots of the bikes. The roll stabilizes quickly for the red bike and shows minor fluctuations as compared to the green bike that shows large oscillations which indicates the green bike following the same trajectory deviates from the path as seen in the Figure 5.11b.

  - Roll rate vs time: The bottom plots in the Figures 5.18 are the roll rate vs time plots of the bikes. These plots for the bikes show that the red bike remains relatively stable whereas for the green bike the roll rate fluctuates heavily. This instability is a major contributor of the overall oscillatory behaviour of the green bike as confirmed by the trajectories shown in the Figure 5.11.

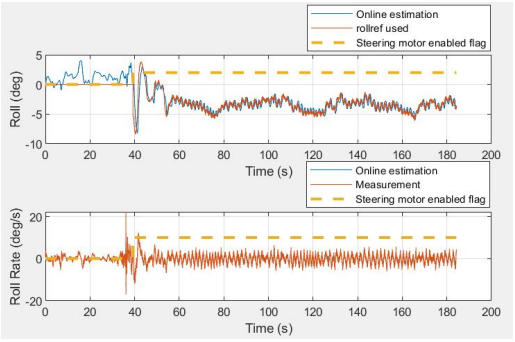

(a) Roll and roll rate vs time for red bike

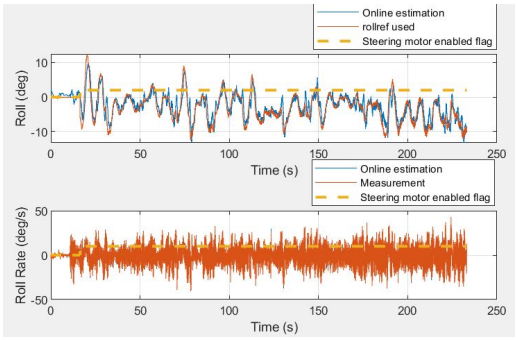

(b) Roll and roll rate vs time for green bike

Figure 5.18: Roll and roll rate vs time of the bikes

- Steering angle vs time: The Figures shown in 5.19 are the steering angle vs time plots of the bikes. The steering angle initially has some fluctuations but reaches a stable state over time as compared to the green bike for which the steering angle shows continuous large oscillations which indicates that the control system is making large corrections causing instability.

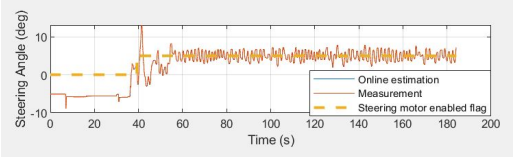

(a) steering angle vs time for red bike

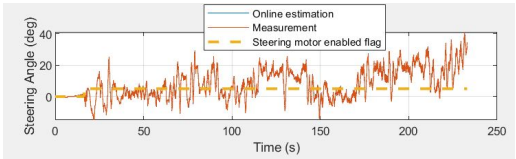

(b) Steering angle vs time for green bike

Figure 5.19: Steering angle vs time of the bikes

6
Conclusions

This chapter comprises of the conclusions gained from the work done in the project.

6.1 Key Findings and Improvements from E-Scooter Testing

This project focused on testing with e-scooters, drawing key conclusions from the experiments conducted.

- The addition of an extra roller allowed the e-scooter to be tested indoors, providing a controlled environment for assessing balance. Indoor tests are crucial for evaluating the stability of the bike or e-scooter.
- The previous steering motor enabled the e-scooter to balance on its own for a certain period of time, but it encountered issues and was replaced by a new motor similar to the ones used in bikes.
- New mount plates were fabricated which were reliable and durable on the longer run as the material used was aluminum instead of glass.
- With the new steering motor, the balance control parameters were adjusted to help the scooter react swiftly in the opposite direction of the roll to maintain stability. However, this adjustment proved inadequate, as the e-scooter was still unable to balance during outdoor tests.
- To enhance the e-scooter's stability, the effective approach is to alter the center of mass (CoM). To accomplish this, extra weight was added to the e-scooter's steering bar. However, this method was not tested to draw definitive conclusions about its effectiveness.

6.2 Challenges and Findings from Testing the Plastic Bike

The plastic bike featured 3D-printed components and hollow tubes for the chassis. We replaced the front wheel, as the previous wheel's bearings were damaged and could no longer rotate smoothly. Some parts had to be reprinted, as 3D-printed components lack the durability of metal parts. Unlike the green and red bikes, the plastic bike didn't have its own control box; instead, it shared one with the green bike. Balancing tests were conducted at Astazero proving ground, where we fine-tuned the balancing controller parameters. The bike was able to balance, though

wiggling was observed. This instability was due to the lightweight plastic structure. Moreover, the wheel alignment was off, and no trajectory tests were conducted.

6.3 Trajectory Comparison: Red vs. Green Bike

During our visit to the Astazero test track, we worked with the green bike to compare its performance with the red bike. While testing, we observed oscillations in the green bike, whereas the red bike followed the reference path without deviation, as shown in the Figure 5.11. A possible reason for this discrepancy could be the control box on the green bike, which was not securely fastened to the chassis and was moving during the test. This movement may have acted as an external disturbance, interfering with the IMU signals and causing the oscillations. Another potential solution to reduce these oscillations is to fine-tune the gains of the balancing controller. Although both the red and green bikes shared the same controller gains, adjustments in the green bike's settings could help eliminate the oscillations.

7

Future Work

This chapter presents potential improvements for the project identified throughout the report.

7.1 Enhanced Testing and Optimization of E-Scooter Stability

- Testing of the CoM Adjustment: Conduct tests on the effectiveness of adding extra weight to the steering bar to alter the center of mass. This could involve both indoor and outdoor tests under varying environmental conditions (e.g., wind, uneven surfaces) to determine optimal weight placement and the extent of stability improvement.
- Refinement of Steering Motor Response: Improve the responsiveness of the new steering motor by further fine-tuning the control parameters.

7.2 Durability Improvements for 3D-Printed Components for the Plastic Bike

Future work could focus on exploring alternative materials for 3D printing to enhance the durability and reliability of components. Investigating stronger materials, such as carbon-fiber-infused filaments, could significantly improve the longevity of parts and minimize the need for frequent reprinting.

A hybrid structure for the plastic bike could be developed by combining 3D-printed parts with metal reinforcements. This approach would strengthen the bike's frame and reduce its flexibility, thereby improving stability and balance. Optimizing wheel alignment and redesigning the frame could address misalignment issues and enhance the bike's ability to handle external disturbances. Revising the geometry of the bike to better accommodate these factors would contribute to stability and better balance.

7.3 Control Box and Tuning of the Gains for the Green Bike

To enhance the performance of the green bike, it is essential to redesign the mounting system for its control box. Implementing a secure and shock resistant mount would prevent the control box from shifting during operation, thereby eliminating disturbances that interfere with IMU readings. This adjustment would ensure stable and reliable data, leading to improved overall performance of the bike.

Exploring individualized gain tuning for each bike could address the varying oscillatory behaviors observed. The green bike demonstrated different performance issues compared to the red bike, its controller parameters should be tailored to its weight, structure, and dynamic characteristics. Fine-tuning these parameters individually for each bike would help optimize their balance and path following capabilities, reducing oscillations and enhancing stability.

Bibliography

[1] Grandview Research, "Bicycle Market Analysis", Grandview Research, [Online]. Available: https://www.grandviewresearch.com/industry-analysis/bicycle-market

[2] Jonathan Keane, "E-Scooter Survey Says Users Drastically Reducing Car Use in European Cities", Forbes, August 25, 2022, [Online]. Available: https://www.forbes.com/sites/jonathankeane/2022/08/25/e-scooter-survey-says-users-drastically-reducing-car-use-in-european-cities/?sh=78dcbcb46e54

[3] European Commission, "Road Safety: Cyclists", February 13, 2023, [Online]. Available: https://road-safety.transport.ec.europa.eu/document/download/e916d096-cdae-4979-8700-0c81db3fbde6_en?filename=ff_cyclists_20230213.pdf

[4] AB Dynamics, "Soft Bicycle 360", [Online]. Available: https://www.abdynamics.com/track-testing/adas-targets/soft-bicycle-360/?utm_source=Internal+contacts+and+distributors%2C+and+NCAP+Motorcycle+webinar+%28combined%29&utm_campaign=d2f7cae928-EMAIL_CAMPAIGN_2024_10_17_02_54&utm_medium=email&utm_term=0_-d2f7cae928-%5BLIST_EMAIL_ID%5D

[5] 4activeSystems, "Crashtest Technology", [Online]. Available: https://www.4activesystems.at/wp-content/uploads/2020/07/18090101-CrashtestTechnology.pdf

[6] Volvo Group, "Heritage: Three-Point Safety Belt", [Online]. Available: https://www.volvogroup.com/en/about-us/heritage/three-point-safety-belt.html

[7] Autobike Project, GitHub Repository, [Online]. Available: https://github.com/Autobike/Autobike

[8] Viewpoint USA, "What is LabVIEW?", [Online]. Available: https://www.viewpointusa.com/labview/what-is-labview/

[9] NI, "Virtual Instrumentation with LabVIEW", [Online]. Available: https://www.ni.com/en/shop/labview/virtual-instrumentation.html?srsltid=AfmBOoriUbrlqgin3uxD-0LcxiWDrwEMI64BLPx85Y3mDpd3uCbIB57F

[10] "Virtual Instruments (VI) in LabVIEW", Electronics Notes, [Online]. Available: https://www.electronics-notes.com/articles/test-methods/labview/vis-virtual-instruments.php

[11] Educative.io, "What is Visual Studio Code?", [Online]. Available: https://www.educative.io/answers/what-is-visual-studio-code

[12] MathWorks, "What is MATLAB?", [Online]. Available: https://se.mathworks.com/discovery/what-is-matlab.html
[13] Peasley, Eric, "An Introduction to Using Simulink", University of Oxford, Department of Engineering Science, 2013.
[14] Gustaver, Magnus, "Biomechanics Study", Chalmers ODR, [Online]. Available: https://odr.chalmers.se/items/a12f689c-fbc1-49e3-9e17-7aedf5673c9f
[15] Image of Hardware Setup 1, [Online]. Available: https://images.app.goo.gl/y9BJG4xfM1wzgteZA
[16] Image of Hardware Setup 2, [Online]. Available: https://images.app.goo.gl/ojebKSHeUwRfudKJA
[17] García-Vallejo, Daniel, Werner Schiehlen, and Alfonso García-Agúndez, "Dynamics, Control, and Stability of Motion of Electric Scooters", Advances in Dynamics of Vehicles on Roads and Tracks, Proceedings of the 26th Symposium of the International Association of Vehicle System Dynamics, IAVSD 2019, August 12-16, 2019, Gothenburg, Sweden. Springer International Publishing, 2020.
[18] SAFER, "Car-Cyclist Crashes in Europe and Identification of Use Cases for Advanced Driver Assistance Systems", [Online]. Available: https://www.saferresearch.com/library/car-cyclist-crashes-europe-and-identification-use-cases-advanced-driver-assistance-systems
[19] European Transport Research Review, [Online]. Available: https://etrr.springeropen.com/articles/10.1186/s12544-024-00654-0

A
Appendix

A.1 CAD Drawings

This chapter contains all the CAD drawings designed using Autodesk Fusion 360. All the dimensions mentioned in these drawings are in millimeter(mm) and contains ISO standards.

A.1.1 Steering motor mount plates

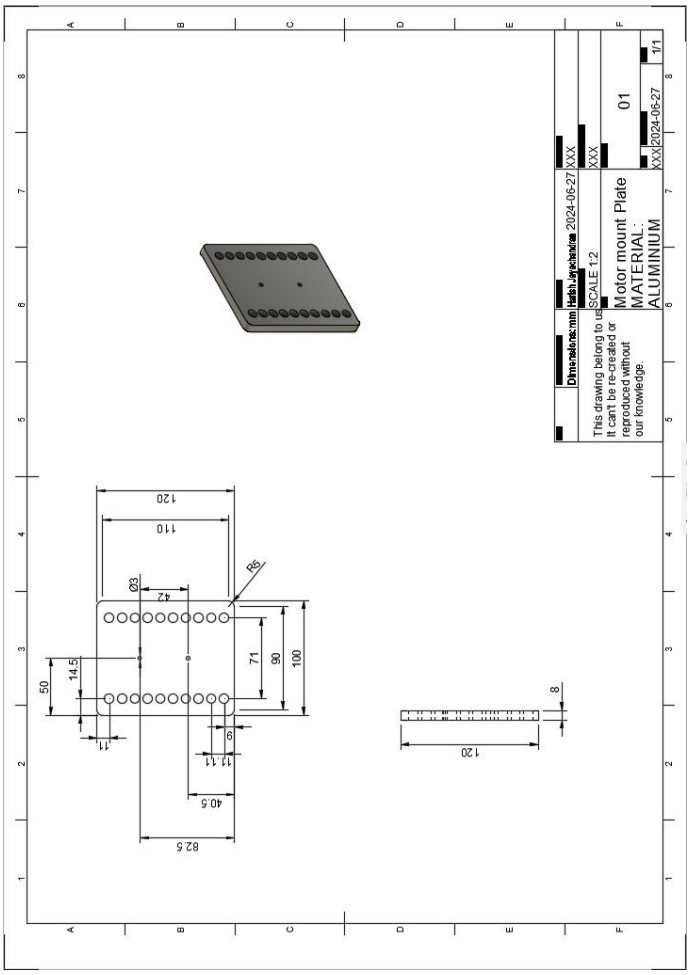

Figure A.1: Drawing of the steering motor mount plate

A.1.2 Outer cylinder for the roller

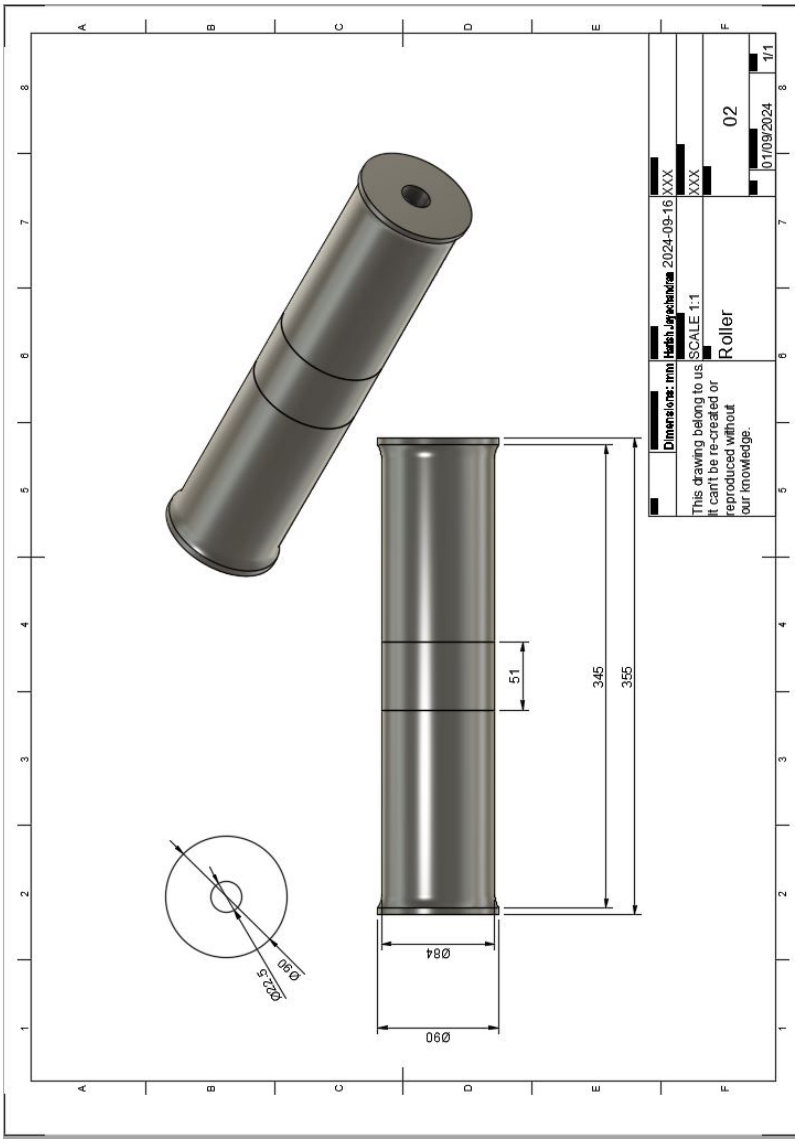

Figure A.2: Drawing of the outer cylinder of the roller

A.1.3 Side supports

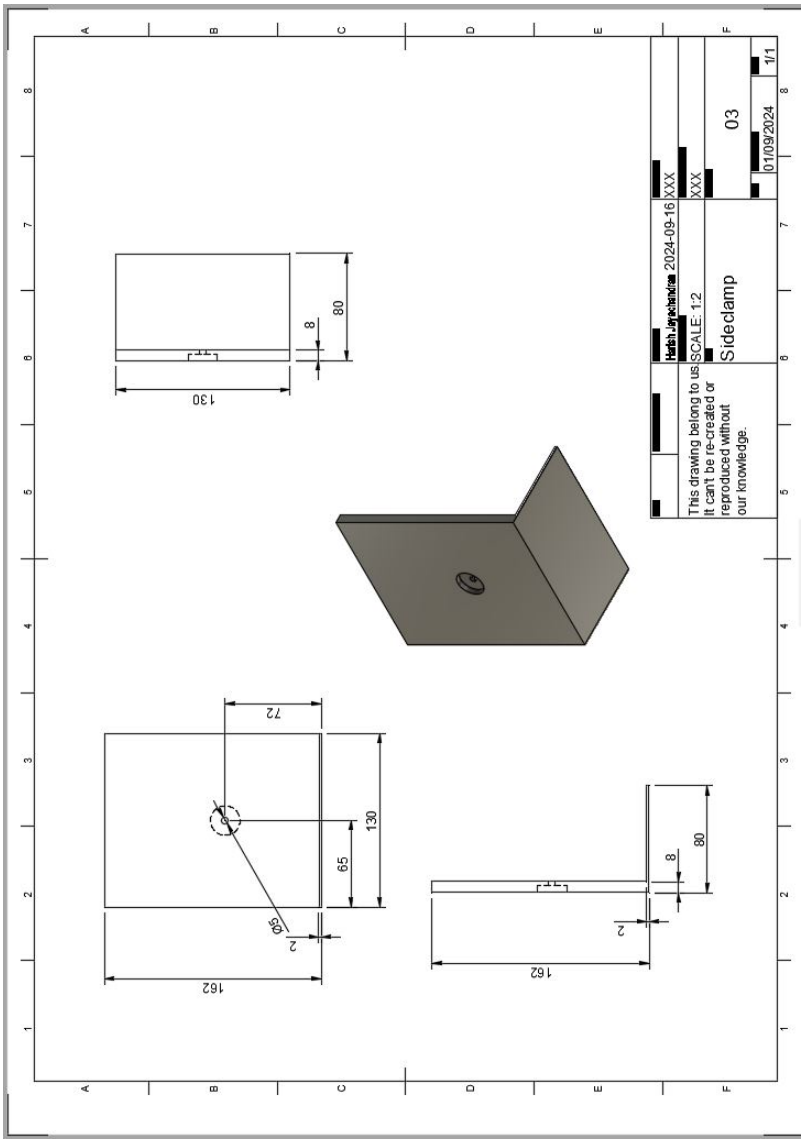

Figure A.3: Drawing of the side support for the roller

A.1.4 Elliptical gear

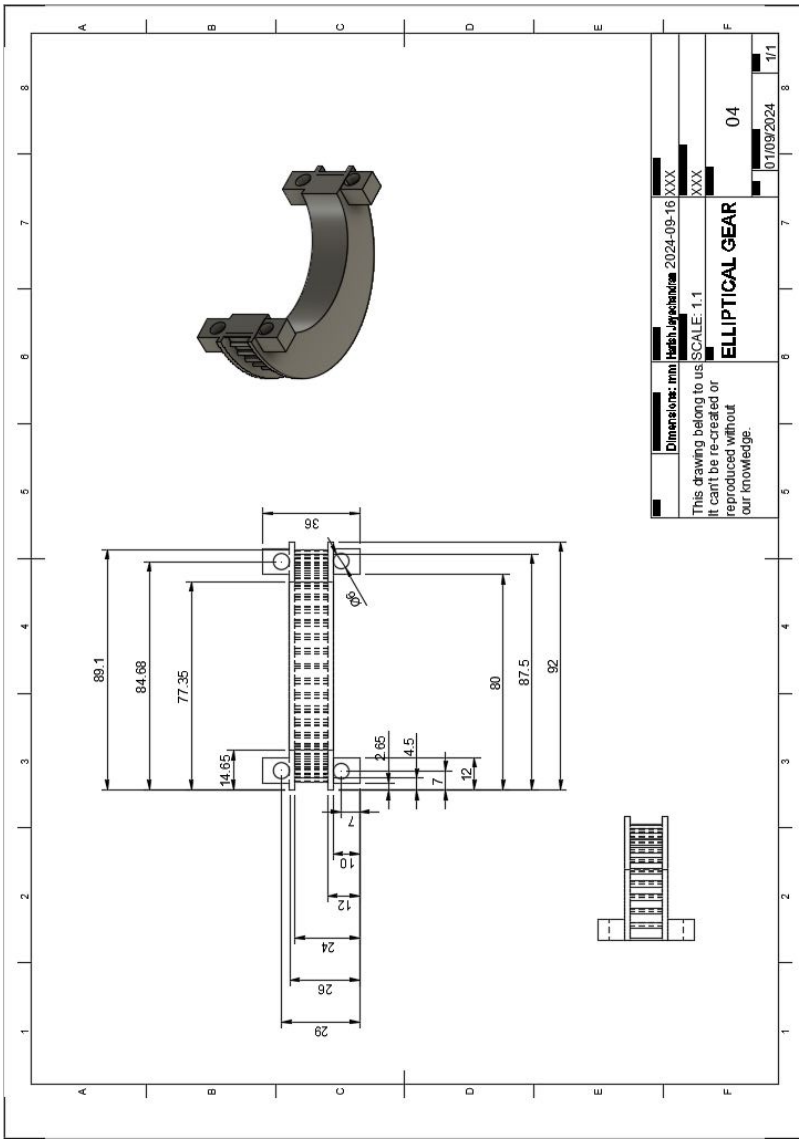

Figure A.4: Drawing of the elliptical gear

DEPARTMENT OF SOME SUBJECT OR TECHNOLOGY
CHALMERS UNIVERSITY OF TECHNOLOGY
Gothenburg, Sweden
www.chalmers.se

CHALMERS
UNIVERSITY OF TECHNOLOGY